On Entangled Singlet Pure Diradicals

Georges Trinquier, Grégoire David, Elohan Veillon, Jean-Paul Malrieu

On entangled singlet pure diradicals

Georges Trinquier,[†] Grégoire David,[‡] Elohan Veillon,[†] and Jean-Paul Malrieu [†*]

[†] Laboratoire de chimie et physique quantiques, IRSAMC-CNRS-UMR 5626, Université Paul-Sabatier (Toulouse III), 31062 Toulouse Cedex 4, France

[‡] Institut des sciences chimiques de rennes, ISCR-CNRS-UMR 6226, Université de Rennes, 35000 Rennes, France

Abstract. This work addresses a class of conjugated hydrocarbons which are expected to be singlet diradicals according to the topological Hückel Hamiltonian, while possibly satisfying full on-bond electron pairing. These systems possess two degenerate singly-occupied molecular orbitals (SOMO), but aromaticity brought by properly-positioned six-membered rings do prevent Jahn-Teller distortions. Density functional theory (DFT) calculations performed on two emblematic examples confirm the strong bond-length alternation in the closed-shell solutions, and the clear spatial symmetry in the open-shell spin-unrestricted determinants, the latter solution always being found of significantly lower energy. Since the SOMOs are here of different symmetry, the wavefunction is free from ionic valence-bond component, and spin decontamination of the unrestricted DFT solutions and wavefunction calculations at CASSCF-plus-2nd-order-perturbation level confirm the expected pure diradical character of such molecules. In contrast to disjoint diradicals, the SOMOs of present systems have large amplitudes on neighbor atoms, and we propose to name them *entangled pure diradicals*, further providing some prescription rules for their design. Additional calculations point out the qualitative contrast between these molecules and the related diradicaloïds.

1. Introduction

The present paper addresses some molecular architectures of alternant conjugated hydrocarbons which can be a priori considered as diradicals,[1-9] *i.e.* preferably described with two singly-occupied molecular orbitals (SOMOs), but which happen to exhibit special properties. Distinguishing between closed-shell and singlet diradicals may turn problematic and requires to clarify the physics taking place between two electrons either in the HOMO-LUMO set, or in the SOMO set.[1-3,9] From the former set, it is always possible to define equivalent orbitals localized on subsets of atoms of different "colors", in the sense given in the alternant world. Then, one may transfer the valence bond (VB) concepts of covalent and ionic components to the ground state wavefunction. As in general this wavefunction is a variable combination of the components, clear distinction between closed-shell and diradical molecules may sometimes prove rather arbitrary. The present work proposes specific architectures free from ionic components. As such, they should be called "pure singlet diradicals", in contrast to most of the so-called diradicals, which accept ionic components, and should therefore be preferably named "diradicaloids".[10]

Beyond this preliminary clarification, this work will consider conjugated hydrocarbons obtained by connecting the outermost atoms of two different odd conjugated polyenyl chains through two aromatic polycyclic units (Scheme 1). Two typical structures were specifically designed for this purpose. Their expected

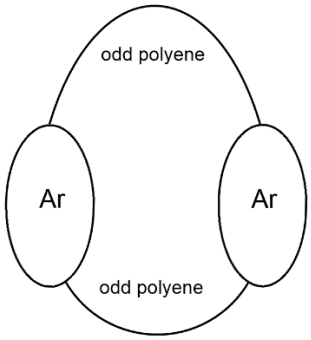

Scheme 1

properties, drawn from simple topological arguments, as well as from chemical intuition, would first suggest to consider them as diradicals. However, these architectures might in principle accept complete electron pairing on double bonds just as well, as they correspond to Kekuléizable graphs, liable to give classical closed-shell molecules. Actually, the topological Hückel Hamiltonian,[11] which considers equal CC bond lengths, predicts for these systems two degenerate SOMOs, of strictly zero energy. In principle, a Jahn-Teller distortion should

take place to remove this degeneracy, but in the proposed designs, such geometry change, because it would favor electron pairing on double bonds throughout almost the entire molecule, would cancel the benefit of aromaticity by destroying Clar's sextets [12] in some bridging six-membered rings. In other words, saving aromaticity in all six-membered rings here compels the systems to remain diradical.

As we will show, in the proposed symmetrical molecules, the two SOMOs are of different irreducible representations. This means that mixing between neutral and ionic components of the ground-state wavefunction is zero, and that these systems behave as pure singlet diradicals. The preference for a singlet multiplicity is here due to the spin polarization mechanism.[6,13,14]

Results of geometry optimizations at density-functional-theory (DFT) level will actually show that, in such systems, closed-shell solutions lose spatial symmetry and exhibit strong bond-length alternation along the polyenyl strings, in agreement with an electron pairing on their bonds, whereas only half of the polycyclic parts retains its entire aromatic character. Even at this bond-alternating geometry, the restricted self-consistent solution is spin unstable, and open-shell spin-unrestricted treatment leads to a lower energy, this minimum-energy conformation keeping spatial symmetry. Methodological limits of the BS-DFT approach have however to be discussed, and we will show that spin decontamination does not change the conclusions - the minimum-energy geometry keeps symmetry. Multiconfigurational wavefunction calculations further support the conclusions of DFT computations. These molecules therefore appear as pure singlet diradical, with entangled SOMOs, and we propose to call such systems *entangled pure diradicals*.

Alternatively, if polyenyl strings have SOMOs of the same symmetry, the saving of aromaticity in the six-membered rings still results in space-symmetry saving, but now the topological Hamiltonian no longer predicts a zero HOMO-LUMO gap, and the BS solution exhibits important ionic component. Such molecules may be considered as classical *diradicaloïds*. The singlet-to-triplet excitation energy is here higher than in the previous series, comfirming the singularity of entangled diradicals.

Organized along these lines, the paper is hence divided into the following sections. After a brief recall on singlet diradicals (Section 2), we will present the two candidates, scrutinizing in particular their topology, chromatic attributes and symmetry properties (Section 3). In Section 4, the results of DFT calculations are given, analyzed, and discussed, with special emphasis on several computational challenges associated to accurate and reliable descriptions of these entities. Next, in Section 4, diradicaloids alternatives are subject of the same attention and treatments, allowing to plainly point the similarities and differences between both types of diradicals. Last, the conclusion section will delineates some general questions about entangled diradicals and

will attempt to provide a comprehensive classification of spin-properties of even alternate conjugated hydrocarbons.

2. A brief recall on singlet diradicals

The molecules possessing a triplet ground state, such as *meta*-xylylene, must definitely be considered as diradicals, their wavefunction requires considering two singly-occupied MOs, as it is clear for the m_s=1 component of the triplet. The distinction between closed-shell molecules and singlet diradicals in organic chemistry is a matter of debate. It is usually recognized that there is no well-defined border between the two types of molecules,[1-9] and a variety of criteria or indices of diradical character have been proposed.[7,15-21]

As well-known from basic studies on single bonds like that in H_2, a same system may go from a closed-shell nature to a diradical nature as soon as the bond is stretched. When does the molecule become diradical ? The question concerns all single-bond breaking processes. The analysis is formulated differently according to the types of MOs used. Expressing the wavefunction in terms of *localized*, atom-centered, orbitals *a* and *b*, the singlet ground-state wavefunction involves a variable mixing between neutral (covalent) and ionic VB components, the neutral (diradical) component taking increasing weight as the bond is stretched.[22] On the other hand, usual bond descriptions rather introduce *delocalized* molecular orbitals, a bonding one, *g*, and its antibonding counterpart *u*. Restricting the wavefunction to a single determinant, with double occupancy of the *g* bonding orbital, imposes equal coefficients to neutral and ionic components. However, the determinant involving double-occupancy of the *u* antibonding orbital plays an increasing role when the bond length is increased, and combining the two closed-shell determinants reduces the weight of ionic VB components. Deciding when the molecule becomes a diradical is arbitrary, quite in contrast with triplet systems, which are of open-shell nature. A qualitative signature of the entrance into the diradical regime might be *spin instability* of the closed-shell wavefunction, *i.e.* the fact that a determinant of lower energy than the spin-symmetry adapted one may be obtained by using non-orthogonal orbitals for the unpaired electrons. This tend to localize them in different regions of space or on different sets of atomic orbitals.

The same discussion applies to molecular systems identified as singlet diradicals. Two electrons may be distributed in nearly-degenerate HOMO and LUMO orbitals, equivalent to the *g* and *u* orbitals of the H_2 problem, or in equivalent localized orbitals *a* and *b*, linear combinations of the above HOMO and LUMO. These equivalent orbitals play the same role as atomic orbitals in H_2. In alternant hydrocarbons, these two equivalent MOs are defined on different sets of atoms, corresponding to opposite colors. In that sense, they

may be considered as localized, despite the fact that they are spread throughout the whole molecular frame - a point discussed in section 3.

The two-electron-in two-orbital problem of the H_2 molecule may be applied to the physics taking place between two electrons distributed on the HOMO and LUMO of extended systems. The excited triplet state of these molecules is *purely* neutral, with one electron in each of these two "localized" orbitals, while their ground singlet state is *predominantly* neutral, with significant ionic contribution partly responsible for the antiferromagnetic coupling of the two electrons. Hydrocarbons with a triplet ground state, such as *meta*-xylylene, are strictly neutral, *i.e.* they are pure diradicals. It is frequently suggested to call "diradicaloids" the systems which have a singlet ground state with a predominantly neutral component. Their closed-shell description is usually subject to spin instability, leading to unrestricted or broken-symmetry (BS) single-determinant solutions.[23-30] These solutions introduce non-zero ionic components, and for this reason are called "diradicaloids", in contrast to "pure diradicals" whose wavefunctions are free from ionic components.[31] In trying to find a criterion to distinguish between closed-shell and diradicaloid systems, the spin-symmetry breaking has the advantage of being a qualitative phenomenon, and not a matter of quantity. However, it is not an absolute criterion, since by varying the exchange correlation potential, a system at a given geometry may move from a stable regime to an unstable one.

A special class of singlet diradicals are disjoint diradicals,[5] where the unpaired electrons occupy remote SOMOs, localized on disjoint sets of atoms, or connected by atoms on which SOMOs have zero amplitudes. The prototype of them is tetramethyleneethene (TME) or diallyle.[32-36] Due to the disjunction of the SOMOs, the coefficient of the ionic component is here strictly zero, at least in a tight-binding Hamiltonian. One may consider such molecules as "pure diradicals", and their antiferromagnetism is due to spin-polarization effects.[16] It is important to notice that the known disjoint diradicals built from conjugated hydrocarbons do not accept on-bond electron pairing - they are not Kekuléizable. Another family of almost pure diradicals are bis(monoradical) systems where the two monoradicals are so far that they no longer interact with each other.[37]

The challenge of the present work is the tentative conception of conjugated alternant hydrocarbons which (i) would be of singlet ground state, (ii) would be Kekuléizable, but (iii) would have zero ionic components. This means that they should have two SOMOs of zero energy in the tight-binding Hamiltonian. Their equivalent localized orbitals should not interact, not because of their distance, but for another reason, namely symmetry. As these systems can in principle be subject to a Jahn-Teller effect,[38] removing the HOMO-LUMO degeneracy, they can regress to closed-shell or standard diradicaloid character. However, from old studies of Chichibabin series,[39-42] and other works,[43-55] one knows that aromaticity in six-membered rings objects to the pairing of unpaired electrons, which may counteract the above Jahn-Teller effect. The present work will exploit this

physical effect in designing candidate molecules which, should they exist, would represent a new class of diradicals that we propose to name *entangled* diradicals, as opposed to *disjoint* diradicals.

3. Candidates and their specifications

This section does not report numerical calculations, it simply calls well-known properties of conjugated hydrocarbons. Most of them have been established in the early days of quantum chemistry from topological tight-binding Hamiltonians, such as Hückel's,[8] Pariser-Parr-Pople's,[56,57] or Hubbard's,[58] all considering only mono-electronic interactions between adjacent carbons.

A) *The two nominees*.

The two compounds selected for this study are pictured in Figure 1. These conjugated hydrocarbons are composed of two linear polyenic radicals, connected to one another by their extremities through aromatic bridges, phenantrene units in the first case, diphenylene units in the second case. The lengths of the polyenic chains are of five and seven –CH– links in the first compound, and three and nine –CH– links in the second one. They will hence be labelled flake **5-7**, and flake **3-9** respectively. Importantly, these chains are attached to atoms of different colors, which avoids a triplet ground state. Additionally, in order to evade steric hindrance, one has introduced sp^3 carbon atoms in CH units inside the conjugate systems, making them partially graphanized. We have checked that this stabilizing chemical change does not affect the properties of the conjugated system, which remains very close to planarity (see the supporting information SI1-SI6). At this point, notice in Figure 1, left, how the molecules accept an on-bond electron pairing, which would tend to suggest closed-shell singlet ground states. A more detailed analysis is necessary to decide which of the two pictures - closed-shell or diradical - is the best electronic depiction.

B) Coloring and symmetry preliminaries.

The molecules here designed and scrutinized hold a remarkable combinations of properties:

(1) They are *alternant* hydrocarbons, since one may attribute one of two colors - say red and blue - to each carbon in such a manner that an atom of a given color is only bonded to atoms of the other color. Said in graph-theory language, the corresponding graph has a chromatic number of two. Practically, this condition is satisfied as soon as the graph is free from odd-numbered rings. In the following, red and blue atoms and coefficients will be labelled by subscripts *r* and *b* respectively (seeing red as *amaranth*, you get back classic starting indexes *a* and *b*).

(2) They have the same numbers of red and of blue carbon atoms, n_r and n_b, respectively.

(3) According to Ovchinnikov's rule, their ground state is of singlet multiplicity.[59] The rule states that the ground-state multiplicity of an alternant hydrocarbon is equal to $|n_r\text{-}n_b|+1$. It has been established from magnetic descriptions of π electron systems, assuming their wavefunctions may be described from a Heisenberg spin-Hamiltonian, with antiferromagnetic couplings between neighbor atoms only.[60-62] In this sense this spin Hamiltonian also keeps a tight-binding character. This model is efficient and may even be used as a quantitative predictive tool,[63] provided that bond-length dependence of interatomic spin coupling has been fitted on *ab initio* calculations of the ethylene molecule.[64] Ovchinnikov's rule may be demonstrated from MO approaches as well, and from Hubbard,[65] or Pariser-Parr-Pople Hamiltonians.[66] It does not require bond lengths to be equal, and, to the best of our knowledge, no counterexample to its predictions has ever been reported.

(4) Alternant hydrocarbons obey the "mirror theorem", formulated years ago by Longuett-Higgins,[67, 68] It establishes a one to one correspondence between bonding φ_i and antibonding φ_i^* orbitals:

$$|\varphi_i\rangle = \sum_{p_r} c^i_{p_r} |p_r\rangle + \sum_{q_b} c^i_{q_b} |q_b\rangle$$

$$|\varphi_i^*\rangle = \sum_{p_r} c^{i*}_{p_r} |p_r\rangle + \sum_{q_b} c^{i*}_{q_b} |q_b\rangle$$

On red atoms, antibonding φ_i^* and bonding φ_i have equal coefficients, whereas on blue atoms, both orbitals have opposite coefficients:

$$c^{i*}_{p_r} = c^i_{p_r}$$

$$c^{i*}_{q_b} = -c^i_{q_b}$$

This is true, in particular, for the HOMO and LUMO of alternant hydrocarbons (labeled φ_h and φ_l respectively). Performing a 45° rotation between these two MOs, one gets an orbital entirely localized on the red atoms

$\varphi_r = (\varphi_l + \varphi_h)/\sqrt{2}$,

and an orbital entirely localized on the blue atoms:

$\varphi_b = (\varphi_l - \varphi_h)/\sqrt{2}$.

These statements remain true when on-bond hopping integrals are not equal, and the definition of red and blue equivalent orbitals is valid for diradicaloïds as well as for the presently-discussed pure diradicals.

(5) Purely topological Hamiltonians are tight-binding Hamiltonians, which consider all on-bond interactions as equal. On our proposed molecules, it can be checked that solutions of the topological Hückel Hamiltonian exhibit two degenerate MOs of zero energy (Figure 2), whereas a gap exists between the HOMO and LUMO in diradicaloïds. It is then rational to consider they are singly-occupied MOs (SOMOs), since

putting two electrons in the same SOMO would increase bi-electronic repulsion. If the existence of the two zero-energy eigenvalues can be obtained numerically from the Hückel Hamiltonian, this can also be established analytically on the back of an envelope, and such a deductive approach also provides the corresponding on-site amplitudes, as detailed below.

Although symmetry-adapted, the two SOMOs run on atoms of different colors, and may therefore be considered as "localized" (or color-localized). From above considerations, the two SOMOS can therefore be localized on red and blue atoms respectively, with their coefficients obeying the eigen-equation

$$h|\varphi\rangle = 0|\varphi\rangle = 0$$

meaning the action of the Hamiltonian on a SOMO kills it. For obvious reasons illustrated in Figure 3, these localized SOMOs can be termed the red and blue SOMOs, labeled ϕ_r and ϕ_b respectively. Let us consider the red SOMO, first. As the action of intersite-hopping operators of the Hamiltonian on its blue atoms sends electrons to their red neighbors, the coefficients of this *red SOMO on blue atoms* are all equal to zero, thus conferring zero amplitude to the blue set. Given that hopping integrals are all equal, this simply means that the sum of coefficients on all red atoms connected to a given blue atom is equal to zero. Similarly, for the *blue SOMO*, the action of *H* on the *red atoms* send electrons to their blue neighbors, conferring zero amplitude to the red set. On our graph one may easily find a SOMO entirely defined on the π atomic orbitals of the red atoms

$$|\varphi_r\rangle = \sum_{p_r} c_{p_r} |p_r\rangle$$

and another one defined on the blue atoms

$$|\varphi_b\rangle = \sum_{q_b} c_{q_b} |q_b\rangle .$$

both being eigenvectors of the topological Hückel Hamiltonian with zero energy. As the red SOMO has zero coefficients on blue atoms, the eigen-equation simply concerns each of the blue atoms, and becomes

$$\sum_{p_r \, bonded \, to \, k_b} c_{p_r} = 0, \forall k_b ,$$

with the summation running over all red atoms chemically linked to the given blue atom.

It is possible to generate straight the corresponding amplitudes without computer aid. For the red SOMO of flake **5-7** (Figure 3, upper right), we begin by fixing arbitrarily the coefficient of a given red atom - for instance a coefficient of +1 on an atom with only two blue neighbors like that at far right. Then the coefficients of second neighbors are all set to -1. Thus progressing along the molecular graph, one only needs to solve by hand very simple linear equations involving at most three coefficients. A similar treatment can be applied to the blue SOMO as well, leading to the so-derived integer coefficients given in Figure 3, lower right, with the

smallest ones being +1 or -1, and the larger ones +5 or -5. For convenience, let us further call "*red polyenyl*" the polyenyl chains bearing more red atoms than blue atoms, *ie* the left pentadienyl and allyl chains in flakes **5-7** and **3-9**, respectively, and "*blue polyenyl*" that with more blue atoms than red ones, *ie* the right heptatrienyl and nonatetraenyl chains in flakes **5-7** and **3-9**, respectively (Scheme 2). As mentioned for flake **5-7**, for the red

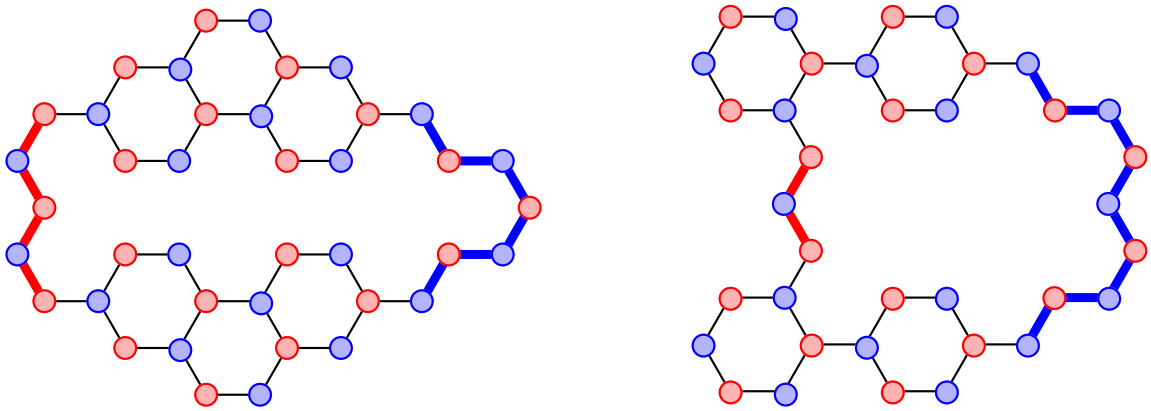

Scheme 2

SOMO, starting with a coefficient 1 on a red atom of the blue polyenyl, one gets coefficients of 5 on red atoms of the red polyenyl. A same ratio is obtained for the blue SOMO. Renormalizing these coefficients would lead to the strict HMO coefficients. Even more, once normalized and summed over the two SOMOs, these numbers can be advantageously confronted to the triplet-state spin densities, as obtained for instance from a RODFT calculation, as shown in Figure 4. The same procedure applied to flake **3-9** leads to integer coefficients from 1 to 4, as detailed in Figure 5. From the integer coefficients of Figure 3, the red symmetrical SOMO ϕ_a is mainly localized at 63 % on the "red" pentadienyl part, at 35 % on the aromatic rings and at 3 % on the "blue" heptatrienyl part. Oppositely, the blue antisymmetrical SOMO ϕ_b is essentially localized at 69% on the "blue" heptatrienyl group, at 29% on the aromatic group, and at 1% on the "red" pentadienyl group. For flake **3-9**, a similar treatment leads to similar trends. For ϕ_b, the repartition of squared coefficients is now 72 %, 27 % and 1 % on the 9-carbon polyenyl, the aromatic part, and the 3-carbon allyl parts respectively. For ϕ_r, these percentages are now 6 %, 36 %, and 42 % respectively, emphasizing here more significant tails on aromatic groups. More generally, as each SOMO is centered on one of the two odd polyene chain with significant

delocalization tails, the position of its center of mass could be easily calculated, as well as the distance between these two centers in terms of mean-CC-bond-length-unit.

(6) The degeneracy of the two SOMOs implies that they do not interact, as $< \phi_r \mid h \mid \phi_b > = 0$, and they are indeed of different symmetries. As can be checked in Figures 2 and 3 for flake **5-7**, ϕ_r is symmetrical with respect to a plane of symmetry perpendicular to the conjugated frame and passing through outermost carbons, while ϕ_b is antisymmetrical with respect to this plane. For flake **3-9** (Figures 2 and 5), ϕ_b is now antisymmetrical with respect to the plane of symmetry, while ϕ_r is symmetrical. We immediately note the crucial tendency that polyenyl chains bearing the *symmetrical* layout of coefficients have always lengths of type ($4n$+1), while those carrying the *antisymmetrical* layout of coefficients have always lengths of type ($4n$-1). More explicitly, in flake **5-7**, the pentadienyl part, mainly borne by ϕ_r, of length 5 (=$4n$+1), is symmetrical, while the heptatrienyl part, mainly borne by ϕ_b, of length 7 (=$4n$-1), is antisymmetrical. In the same way, in flake **3-9**, the nonatetraenyl chain, borne by ϕ_b, of length 9 (=$4n$+1) is symmetrical, while the allyl chain, borne by ϕ_r, of length 3 (=$4n$-1) is antisymmetrical (see Figures 2, 3, and 5). A key point, here, is that the *difference* between the lengths l_1 and l_2 of the two odd linear chains (Scheme 3) is and must be equal to $4m$+2,

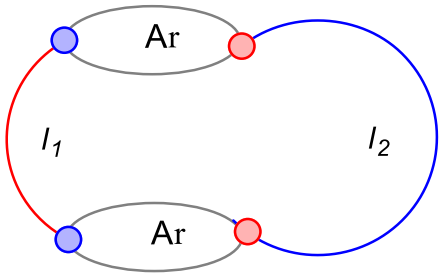

Scheme 3

or equivalently that the *sum* of their lengths is a multiple of 4. Satisfying this condition precisely defines the "entangled diradicals", in particular differentiating them from diradicaloid species - a point that will be addressed subsequently.

(7) Other types of graphs exhibit two degenerate SOMOs, but they are deeply different from present molecular skeletons. Those who are of triplet ground state, such as trimethylene methane (TMM), or *meta*-xylylene, are not Kekuléizable, and have a difference $|n_r - n_b|$=2. Their SOMOs run on atoms of the *same color*, and their coefficients can still be obtained according to the above recipe. Another family of graphs have two SOMOs of opposite colors, namely the so-called *disjoint* diradicals, mentioned in the preceding section. They

can be defined by connecting two radical moieties through atoms where SOMOs have zero amplitudes. For instance, TME is composed of two allyl radicals connected by their central carbons, where the SOMOs have a node.[5,28,32] SOMO disjunction satisfies the relation $\langle \varphi_r | h | \varphi_b \rangle = 0$, at least for a tight-binding Hamiltonian. Disjoint diradicals are expected to be singlets, according to Ovchinnikov's rule, but with a small singlet-to-triplet gap.

(8) The SOMOs of our compounds are not disjoint but *entangled*. A given SOMO has here non-negligible coefficients on atoms connected to those where the other SOMO has also non-negligible coefficients (see Figure 2). Unlike in disjoint diradicals, nullity of the interaction between the two orbitals is not due to their spatial separation.

(9) Referring to the physical effects contributing to antiferromagnetism in molecules,[5,69] in magnetic systems, the preference for singlet ground state is usually due to the so-called "kinetic exchange", *i.e.* to the stabilizing effect of the "ionic" component of the wavefunction. Here, we extend the valence bond vocabulary, calling *neutral* the configuration where the two SOMOs bear a single electron, and *ionic* those where the two electrons occupy the same SOMO. The dominant VB component is neutral, and ionic components, which are pure singlets, are only present in the singlet state. The resulting antiferromagnetic contribution may be perturbatively expressed as

$$\varepsilon_{KE}^{(2)} = -\frac{4\langle \varphi_r | h | \varphi_b \rangle^2}{\Delta E_{NI}},$$

where the denominator represents the energy difference between neutral and ionic configurations, while the numerator expresses their interaction. This contribution is almost zero in disjoint diradicals and *strictly* zero if the SOMOs are of different spatial symmetries, as in present systems. In this case, the physical effect stabilizing the singlet state is the spin polarization of the other π MOs and of the σ bonds.[14,15,69] The unpaired electrons of opposite spins, being located on different sets of atoms (red or blue), create an "exchange field" on the electrons of the closed shells and polarize them, the α spin electron of a closed shell feels less repulsion by the unpaired electron of α spin than does the β spin electron of the same shell. The spin orbitals of the closed shell react to this difference and become slightly different, as manifest in UDFT treatments. The process stabilizes the energy.

(10) One should also consider possible symmetry losses and Jahn-Teller distortions. While disjoint diradicals cannot accept electron pairing on double bonds, *i.e.* a Kékulé (or Lewis) writing, our graphs do so, as manifest from Figure 1. Actually, when two degenerate orbitals appear at the Fermi level, one expects a Jahn-Teller distortion will stabilize, as a first-order effect, one of the two orbitals and destabilize the other one, so that the system will accept to become closed-shell with double occupancy of the stabilized orbital. While

disjoint diradicals do not accept such stabilizing geometry change, the here-proposed entangled diradicals do so. They are in principle subject to such distortion, indeed, as single and double bonds can be drawn on the corresponding graphs, insuring perfect on-bond electron pairing, and a closed-shell wave function. Example of such Jahn-Teller distortion are C_{4n} rings, which exhibit entangled SOMOs when bond lengths are equal. In this ideal geometry, they may be seen as perfectly entangled diradicals, but bond-length alternation stabilize them and make them return to a closed-shell wavefunction.[1-9] Our graphs *a priori* do accept such distortion, with bond-length alternation in the odd chains and one aromatic subunit, as pictured in Figure 1, the system losing symmetry and diradical character, and the polyenyl chains entering closed-shell organization. In present compounds, a key point is that bond alternation here destroys aromaticity on at least two six-membered rings. Yet, it has been deduced from DFT calculations that two radical regions cannot be fused into a closed-shell as long as the price to pay is the loss of two or more Clar sextets.[43,44] While *para*-xylylene is a closed shell molecule,[70,71] higher analogs, from Chichibabin's R_2C-$(C_6H_4)_2$-CR_2,[40] to Muller's R_2C-$(C_6H_4)_3$-CR_2[41,42] become more and more diradical as quinonization of two or more benzene rings proves too costly energetically. Quantum chemical calculations have evaluated the six-membered ring aromatic contribution at around 20 kcal/mol,[72] and reluctance to loose this benefit might force the molecular architecture to keep symmetry and entangled diradical character.

The design of the two architectures presented and briefly described in the preceding section was of course governed by this preliminary knowledge, as well as by trial explorations. As these molecules *a priori* accept two deeply different descriptions and wavefunctions, variational calculations, with complete geometry optimizations, are expected to take into account pro-and-con arguments and deliver a decision to this dilemma.

4. Numerical study

A- Standard DFT results

Two representations of these molecules are in competition. If the geometry presents a strong bond alternation, the wavefunction should be of closed-shell character and should be approached by closed-shell standard calculations. In geometries keeping the axial plane symmetry, the wavefunction should be of open-shell character, and should be approached through unrestricted treatment, at least in a first step. One may optimize the geometries of either a closed-shell determinant or of an m_S=0 BS determinant. To this end, RDFT and UDFT calculations were carried out. They were performed using the B3LYP functional and standard 6-311G** basis set, as implemented in the Gaussian 09 software suite.[73] Geometries were optimized with

gradients better than 10^{-5} au, and harmonic vibrational frequencies were systematically calculated to insure that real minima were obtained. These treatments led to the following main features:

(1) The closed-shell solution converges on a geometry leaving the axial plane of symmetry, in which the linear polyenic parts exhibit strong bond alternation, and one of the two polycyclic units keeps its aromatic character while the other one is strongly quinonized.

(2) The spin-unrestricted treatment keeps the axial plane of symmetry, with the polyenic chains no longer showing bond alternation and more reflecting polyenyl radicals, and with now both polycyclic units exhibiting aromatic geometry (see Figure 1, middle). This solution has significantly lower energy than the former one, as shown in Table 1, which gives the relative energies calculated for various solutions, together with a recall of the structural features of our two compounds.

A compact measure of geometrical trends can be obtained by dividing bonds into four groups, namely the long and short polyenyl chains, the polycyclic part supposed to remain aromatic, and the one which quinonizes in the closed-shell solution. Table 2 reports the mean bond lengths within each group, together with their corresponding standard deviations (a complete list of optimized bond lengths is given in the supporting information SI7). This latter quantity is always smaller in the BS solution, for which bond lengths are rather uniform. More specifically, Figures 6 and 7 visualize bond-length changes occurring from BS geometries to closed-shell ones. The points close to the diagonal correspond to those phenyl groups remaining aromatic in the closed-shell solution. The points *above* the diagonal concern those bonds that are formally *single* - hence longer - in the closed-shell picture. The points *below* the diagonal concern those bonds that are formally *double* - hence shorter - in the closed-shell picture. It is conspicuous that in the closed-shell solution the two aromatic systems are different, one remaining composed of two regular phenyl units, while the other is subject to strong quinonization of diphenylene groups. Lateral chains exhibit strong bond alternation, and obviously there exist two degenerate bond-alternating closed-shell solutions, while the unrestricted solution is unique, with its two-fold axis. If closed-shell minima were lower than open-shell minima, this symmetrical geometry would be seen as a saddle point between these minima, which is not the case.

The optimized geometries of the BS m_s=0 solutions exhibit small bond-length differences for conjugated CC bonds. Spatial symmetry is kept, and surprisingly enough the energy is much lower (by 10 kcal/mol) than that of the closed-shell function. Comparing BS m_s=0 energies at diradical geometry with closed-shell energies at closed-shell geometry is not fair, since the physics involved in the two treatments are not the same. The BS calculation treats, at least approximately, some correlation between the two electrons of the HOMO-LUMO subset (neutral/ionic ratio components), and the spin-polarization of the other electrons, which may be

considered as an exchange correlation between the electrons of the SOMOs and the electrons of the almost-closed shells. Fixing to one the neutral/ionic VB component ratio, the closed-shell treatment ignores the correlation between the two upper-energy electrons and their spin correlation with the core electrons. One may nevertheless wonder whether a spin-symmetry breaking occur at closed-shell geometries.

Indeed, BS m_s=0 solutions are found at these geometries, but they remain higher than the same solution for the diradical symmetry by around 4 kcal/mol (see Table 1). Here, the two geometries are treated with the same methodology, and the energy difference becomes relevant. Still rather large, this quantity seems to confirm our speculation: the system resists to any Jahn-Teller distortion and prefers to keep pure diradical character. One might further wonder whether a barrier could take place between the two geometries. Figure 8 picture the section of the potential energy surface corresponding to a linear synchronous transit between the two minima (for the moment, ignore the dashed curves). Clearly, there are no barriers nor humps in these paths, which further illustrate the high instability of closed-solutions at BS geometries, and the instability of BS m_s=0 and m_s=1 solutions at closed-shell geometries. Not unexpectedly, the singlet-to-triplet gaps remain low at diradical geometries (≈ 1 kcal/mol).

B- Methodological scrutiny

One may first wonder whether similar results would be obtained from different exchange-correlation potentials. We have repeated the calculations with the M06-2X potential, which is supposed to be relevant for the study of open-shell systems.[74,75] As can be seen in Figure 8 (dashed curves), the main alteration concerns energy differences between BS m_s=0 and the closed-shell solutions, larger for the M06-2X potential than for B3LYP, certainly due to the larger part of HF exchange in M06-2X.

These calculations suffer from the spin-contaminated character of their wavefunctions. This defect has been considered by various authors, and spin decontamination procedures have been proposed. The most popular one is the Yamaguchi correction, which exploits the mean values of the S^2 operator for different spin-polarized determinants.[76] Actually, spin contamination has different origins, as it comes from both (*i*) mixing between magnetic orbitals, which introduces some ionic components in the wavefunction, and (*ii*) from the spin polarization of the "core" MOs under the exchange field of unpaired electrons. The two effects act oppositely on $<S^2>$, the first effect diminishes it, while the second one increases it. The use of a unique correction to treat the two effects is not grounded and may lead to irrelevant values of the singlet to triplet energy gap.

Methodological efforts have been produced to reach reliable estimates of the spin-decontaminated energy. The proceed by breaking up the main corrections to magnetic coupling between unpaired electrons into (*i*) direct exchange (ferromagnetic), (*ii*) kinetic contribution coming from the mixing between neutral and ionic

valence components of the wavefunction, and (*iii*) spin-polarization of core electrons. It is possible to identify these three contributions through constrained DFT calculations, and a rational procedure to eliminate any spin contamination bias has been recently proposed.[77,78] Applied to flake **5-7**, this procedure led to a difference between the spin-decontaminated energies of closed-shell and diradical in their optimized geometries, of 2.2 kcal/mol in favor of the diradical. This is close to the value given by direct comparison of the BS m_s=0 solutions, and in view of this agreement, spin decontamination has not been repeated on other hereafter reported systems.

C- Difficulty of wavefunction calculations

Further evaluation of energy differences between diradical and bond-alternating geometries may proceed through wavefunction calculations. The simplest treatment would consist in mean-field Hartree-Fock (HF) calculations, where a same spin-instability phenomenon takes place, even more dramatically than in DFT. Subjected to such treatment, bond alternation of closed-shell solutions is increased, leading to values close to the ideal limit around 1.35/1.45-Å, as evidenced from the comparatives plots given in the supporting information SI8 and SI9.

Multi-configurational wavefunction calculations enable to avoid the symmetry-breaking problem. Since the diradical ground state requires a two-determinant description (two electrons in two SOMOs), the corresponding description of the closed-shell geometry must be a complete active space (CAS) with two electrons in the HOMO/LUMO set. This CAS-SCF(2,2) is the minimal-balanced description. At this stage, the BS m_s=0 structure of flakes **5-7** and.**3-9** is more stable than the closed-shell one by 3.5 and 1.7 kcal/mol respectively. Post-CAS correlation effects was further treated at NEVPT2 second-order perturbative level, which, in contrast to CASPT2, is parameter free.[79,80] The diradical geometries of flakes **5-7** and **3-9** are then more stable than the closed-shell ones by 2.6 and 3.1 kcal/mol for flakes **5-7** and **3-9** respectively. The results of this treatment are consistent with those of BS-DFT approach, before and after spin-decontamination.

These wavefunction results must be considered critically since a previous work devoted to C_{4n} rings has shown that the relevance of CAS(2,2)+PT2 or NEVPT2 for such systems may be questioned.[81] Spin polarization (or spin correlation) plays a key role in both geometries, and another previous work has demonstrated that the spin-polarization phenomenon is cooperative, as there is positive interference between spin polarizations of the various closed-shell orbitals.[82] According to this work, a correct treatment would require performing a full π valence CASSCF calculation, followed by a 2nd-order perturbation. Such a calculation cannot be performed for our molecules, the π system of which involves more than 30 electrons.

5. Parent diradicaloid architectures

A key point in our explorations is the symmetry of polyenyl SOMOs, since their degeneracies are precisely due to their symmetry difference. As stated above, in the proposed architectures, the two polyenyl lengths were of $4n+1$ and $4m-1$ types, respectively, meaning their SOMOs are of different symmetries with respect to a plane orthogonal to the molecular plane. One may wonder whether similar architectures with polyenyl strings of the same type (say $4n+1$) would behave similarly. To this end, architectures analogous to flakes **5-7** and **3-9**, where polyenyl SOMOs have now the same symmetry, have been studied through the same approaches as in Section 4. These are flakes **5-5** and **3-7** (Figure 9). Again, to preserve a singlet ground state, the chains are attached to atoms of different colors as in scheme 3. For these systems, the HOMO and LUMO of the topological Hamiltonian are no longer degenerate, being separated by 0.17 |β|, and 0.21 |β| for the two systems respectively (β is the hopping integral between adjacent atoms). Is this qualitative difference in symmetries and in mono-electronic spectra correlated with significant differences in the properties predicted by the same DFT treatments applied to the two previous diradicals ?

Here again, the lowest energy is obtained from a broken-spin symmetry wavefunction, keeping spatial symmetry and saving the aromatic character of six-membered rings (Table 3). These systems are however deeply different from the previous ones. While it is still possible to write on-bond electron pairing to the price of formal space symmetry breaking (Figure 9, left), it appears that closed-shell solutions here *no longer exhibits bond-length alternation*, and keep full symmetry with respect to the central perpendicular plane, like the BS solution, as illustrated in Table 4 and Figures 10 and 11 (again, for a complete list of calculated bond lengths, see the supporting information SI10). Such closed-shell geometry suggests seeing the corresponding electronic structure as a resonance between two mesomeric forms, just as benzene can be written as a mean structure between two Kekulé forms (Scheme 4). An important feature not to be missed in Figures 10 and 11 is that for these closed-shell geometries, both left and right six-membered rings exhibit a tendency - moderate, but clear - to quinonization, *i.e.* a shortening of "vertical" bonds and a lengthening of the "oblique" ones. In a way, the closed-shell symmetrical geometry would be also consistent with two radicals on the polyenyl strings, although the solution is of closed-shell character. In summary, both closed-shell and BS m_s=0 geometries are here symmetrical and very close together - a feature quite distinctive from the previous series.

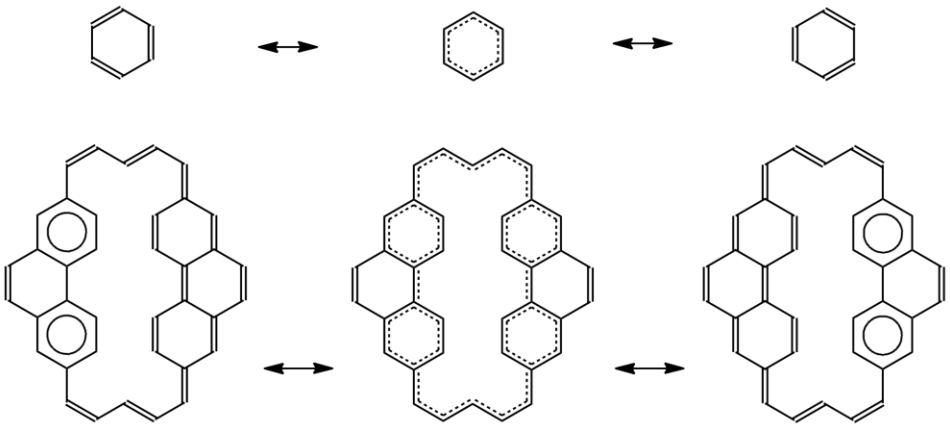

Scheme 4

Let us further compare spin operator mean values, $<S^2>$, for BS solutions in the two series. $<S^2>$ is strictly equal to one for a determinant with a closed-shell core, two orthogonal open shells, and m_s=0 value. It deviates from one when variational BS calculations are performed. As recalled in Section 3, two opposite effects contribute to this deviation. On one hand, spin-polarization of core orbitals increases $<S^2>$, while on the other hand, non-orthogonality of variational magnetic orbitals, by mixing covalent and ionic VB components, diminishes $<S^2>$. In flakes **5-7** and **3-9**, due to SOMO symmetries, there is no ionic component in the BS solution, so that deviation from one of $<S^2>$ is only due to spin polarization. As this effect introduces components with four open shells, $<S^2>$ is expected to be larger than one, and it is actually calculated to be so, as shown in Table 1, bottom. In contrast, for flakes **5-5** and **3-7**, $<S^2>$ is smaller than one (cf Table 3, bottom). Here, spin polarization of core orbitals is also present in BS m_s=0 solutions, and this small value of $<S^2>$ points important mixing between neutral and ionic component in the singlet ground state.

The HOMO-LUMO gap is here sufficient to prevent a Jahn-Teller effect in favor of bond alternation. As shown in Table 10, energy differences between BS m_s=0 and closed-shell solutions are lower than in the previous flakes (3 *vs* 10 kcal/mol), and energy differences between the two geometries calculated with the same BS formalism are also much lower than those of the previous entangled pure diradicals. A CAS(2,2)+NEVPT2 treatment also gives almost the same energy, within 0.5 kcal/mol, to BS and closed-shell geometries. Finally, singlet-to-triplet excitation energies are here significantly larger than in the former architectures (5 *vs* 1 kcal/mol), as triplet geometries are expected to be closer to those of pure diradicals.

The difference between entangled pure diradicals and diradicaloids can also be related to the parity of their peripheral total lengths (consider for instance the inner periphery). In all cases, by construction, each of the two aromatic bridges runs over an even number of carbon atoms. As the sum of polyenyl conjugated centers

are 4*n* and 4*n*+2 for entangled and diradicaloid cases respectively, so are the lengths of their corresponding total closed circuits, as summarized in Table 5. These pseudo annulenes are therefore associated to antiaromatic and aromatic lengths respectively. From the antiaromatic path of entangled systems, one expects clear bond alternation, while from the aromatic path of diradicaloids, one expects full symmetry and equal bond lengths. The latter trend is rather in line with the above observations. On the other hand, if entangled diradicals keep symmetry and decline bond alternation despite their 4*n*-site periphery, this is obviously due to the presence of flanking aromatic six-membered rings within these anti-aromatic C_{4n} annulenes.

6. Conclusion

We have identified a specific type of singlet diradical in the world of alternant conjugated hydrocarbons. Let us further try to establish some schematic landscape or typology of these hydrocarbons. According to Ovchinnikov's rule, color count enables one to distinguish between singlet, doublet (radicals) and triplet architectures. Among singlet ones, one can distinguish between those who accept a Kekulé-type electron pairing - the large majority - and those who do not. The later are disjoint diradicals, with a wavefunction free from ionic components, and spatially disjoint SOMOs. Most of Kekuléizable singlet molecules are correctly described through a closed-shell single determinant, but many of them exhibit some diradical character. One can define as diradicaloïds the molecules whose wavefunctions are indeed predominantly diradical while exhibiting significant ionic components. The existence of spin-instability of the closed-shell determinant could thus define the entrance in diradical regime, while suitable quantitative features of the BS solution would further provide some measure of this diradical character. The here-presented entangled pure diradicals are Kekuléizable but they must be considered as pure diradicals since their wavefunction is free from ionic components, as in disjoint diradicals. In contrast to them, however, their SOMOs are spatially entangled. Finally, we propose in Figure 12 a tentative of typology which helps to position the present entangled species within the diradical realm.

From an epistemic point of view, our research was guided by simple arguments established long ago from topological models, and makes an heuristic use of rather primitive tools. Although these tools, with resulting associated theorems, are rarely taught to chemistry students, they nonetheless keep strong predictive power. Topology, parity and symmetry appear here as determining features, as they do in Woodward-Hoffmann rules.

The present work has only proposed two examples of entangled pure singlet diradicals. Their conception follows the rather intuitive building logics pictured in Scheme 1. One may wonder whether other types of singlet Kekuléizable frames may present the same properties. An ensuing article will soon furnish deeply different

molecular architectures behaving as the present systems. It will further consider some remaining questions: (i) what are the topological conditions to have strictly-degenerate SOMOs in singlet systems ? (ii) is this condition sufficient to have entangled pure singlets ? (iii) is symmetry-keeping compulsory ? (iv) what is the role of aromaticity saving in the preference for pure diradical character ?

Last, a few words about specific potential properties of the present molecules. One of them is the exceptionally low singlet-to-triplet energy gap. Besides, their ions should have interesting properties, as ionization may concern one SOMO or the other. As a consequence, these ions should have close energies and different physical content. Due to spatial localization of the SOMOs, the ions differ by interchange of charge and spin between the two sides of the molecule. A small external electric field could then flip the system from one state to the other, the molecule behaving as an electrically-addressable magnetic device - a speculation confirmed by preliminary calculations.

References

(1) Salem, L.; Rowland, C. The electronic properties of diradicals. *Angew. Chem. Int. Ed.* **1972**, *11*, 92-111.

(2) Borden, W. T. in *Diradicals*, ed. W. T. Borden, Wiley-Interscience, New York, 1982, pp. 1-72.

(3) Fukui, K.; Kazuyoshi, T. A theoretical study on biradicals. I. Theoretical characteristics of biradicals. In: *Frontier Orbitals and Reaction Paths: Selected Papers of Kenichi Fukui*; World Scientific, 1997, 333-340.

(4) Sun, Z.; Wu, J. Open-shell polycyclic aromatic hydrocarbons. *J. Mater. Chem.* **2012**, *22*, 4151-4160.

(5) Abe, M. Diradicals. *Chem. Rev.* **2013**, *113*, 7011-7088.

(6) Malrieu, J.-P.; Caballol, R.; Calzado, C. J., De Graaf, C.; Guihéry, N. Magnetic interactions in molecules and highly correlated materials. *Chem. Rev.* **2014**, *114*, 429-492.

(7) Nakano, M. *Excitation energies and properties of open-shell singlet molecules*, Springerbriefs in molecular science, Springer, Cham, 2014.

(8) Nakano, M. Electronic Structure of open-shell singlet molecules. Diradical character viewpoint. *Top. Curr. Chem.* **2017**, *375*, 47.

(9) Stuyver, T.; Chen, B.; Zeng, T.; Geerlings, P.; De Proft, F.; Hoffmann, R. Do diradicals behave like radicals ? *Chem. Rev.* **2019**, *119*, 11291-11351. This work also reviews various indices of "radicalarity" proposed in the literature.

(10) *Diradicaloids*, edited by Jishan Wu, Jenny Stanford Publishing, Singapore, 2022.

(11) Hückel, E. Zur quantentheorie der doppelbindung. *Z. Physik* **1930**, *60*, 423-456.

(12) Clar E., *Polycyclic Hydrocarbons*; Academic Press: London, 1964; Vol. 1, p. 2.

(13) Kollmar, H.; Staemmler, V. Violation of Hund's rule by spin polarization in molecules. *Theor. Chim. Acta* **1978**, *48*, 223-239.

(14) Karafiloglou, P. The double (or dynamic) spin polarization in π diradicals. *J. Chem. Educ.* **1989**, *66*, 816-818.

(15) Horbatenko, Y.; Sadiq, S.; Lee, S.; Filatov, M.; Choi, C. H. Mixed-reference spin-flip time-dependent density functional theory (MRSF-TDDFT) as a simply yet accurate method for diradicals and diradicaloids. *J. Chem. Theory Comput.* **2021**, *17*, 848-859.

(16) Doehnert, D.; Koutecky, J. Occupation numbers of natural orbitals as a criterion for biradical character. Different kinds of biradicals, *J. Am. Chem. Soc.* **1980**, *102*, 1789-1796.

(17) Head-Gordon, M. Characterizing unpaired electrons from the one-particle density matrix. *Chem. Phys. Lett.* **2003**, *372*, 508-511.

(18) Voigt, B. A.; Steenbock, T.; Herrmann, C. Structural diradical character. *J. Comput. Chem.* **2019**, *40*, 854-865.

(19) Ramos-Cordoba, E.; Salvador, P. Diradical character from the local spin analysis. *Phys. Chem. Chem. Phys.* **2014**, *16*, 9565-9571.

(20) Rivero, P.; Jiménez-Hoyos, C. A.; Scuseria, G. E. Entanglement and polyradical character of polycyclic aromatic hydrocarbons predicted by projected Hartree-Fock theory. *J. Phys. Chem. B* **2013**, *117*, 12750-12758.

(21) Jung, Y.; Head-Gordon, M. How diradicaloid is a stable diradical ? *Chem. Phys. Chem* **2003**, *4*, 522-525.

(22) Angeli, C.; Cimiraglia, R.; Malrieu, J.-P. Non-orthogonal and orthogonal valence-bond wavefunctions in the hydrogen molecule: the diabatic view. *Mol. Phys.* **2013**, *111*, 1069-1077.

(23) Pople, J. A.; Nesbet, R. K. Self-consistent orbitals for radicals. *J. Chem. Phys.* **1954**, *22*, 571-572.

(24) Berthier, G. Configurations électroniques incomplètes. Partie I. La méthode du champ moléculaire self-consistent et l'étude des états à couches incomplètes. *J. Chim. Phys.* **1954**, *51*, 363-371.

(25) Lineberger, W. C.; Borden, W.T., The synergy between qualitative theory, quantitative calculations, and direct experiments in understanding, calculating, and measuring the energy differences between the lowest singlet and triplet states of organic diradicals. *Phys. Chem. Chem. Phys.* **2011**, *13*, 11792-11813.

(26) Ginsberg, A. P. Magnetic exchange in transition metal complexes. 12. Calculation of cluster exchange coupling constants with the Xα-scattered wave method. *J. Am. Chem. Soc.* **1980**, ***102***, 111-117.

(27) Noodleman, L. Valence-bond description of antiferromagnetic coupling in transition metal dimers. *J. Chem. Phys.* **1981**, *74*, 5737-5743.

(28) Takatsuka, K.; Fueno,T.; Yamaguchi, K. Distribution of odd electrons in ground-state molecules, *Theor. Chim. Acta* **1978**, *48*, 175-183.

(29) Yamaguchi, K.; Fukui, H.; Fueno, T. Molecular orbital (MO) theory for magnetically interacting organic compounds. Ab-initio MO calculations of the effective exchange integrals for cyclophane-type carbene dimers. *Chem. Lett.* **1986**, *15*, 625-628.

(30) Yamaguchi, K.; Okumura, M.; Takada, K.; Yamanaka, S. Instability in chemical bonds. II. Theoretical studies of exchange coupled open-shell systems, *Int. J. Quantum Chem.*, **1993**, *48*, 501-515.

(31) Nakano M.; Fukuda, K.; Ito, S.; Matsui, H.; Nagami, T.; Takamuru, S.; Kitagawa, Y.; Champagne, B. Diradical and ionic character of open-shell singlet molecular systems. *J. Phys. Chem. A* **2017**, *121*, 861-873.

(32) Dowd, P. Tetramethyleneethane. *J. Am. Chem. Soc.* **1970**, *92*, 1066-1068.

(33) Filatov, M.; and Sason Shaik, S. Tetramethyleneethane (TME) diradical: experiment and density functional theory reach. *J. Phys. Chem. A* **1999**, *103*, 8885-8889.

(34) Pozun, Z. D.; Su, X.; Jordan, K. D. Establishing the ground state of the disjoint diradical tetramethyleneethane with quantum Monte Carlo. *J. Am. Chem. Soc.* **2013**, *135*, 13862-13869.

(35) Barborini, M.; Coccia, E. Investigating disjoint non-Kekulé diradicals with quantum Monte Carlo: the tetramethyleneethane molecule through the Jastrow antisymmetrized geminal power wave function. *J. Chem. Theory Comput.* **2015**, *11*, 5696-5704.

(36) Veis, L.; Antalík, A.; Legeza, O.; Alavi, A.; Pittner, J. The intricate case of tetramethyleneethane: a full configuration interaction quantum Monte Carlo benchmark and multireference coupled cluster studies. *J. Chem. Theory Comput.* **2018**, *14*, 2439-2445.

(37) Rosenboom, A.; Taube, F.; Teichmeier, L.; Villinger, A.; Reinhard, M.; Demeshko, S.; Bennati, M.; Bresien, J.; Corzilius, B.; Schulz, A. Rational design of a phosphorus-centered disbiradical. *Angew. Chem. Int. Ed.* **2023**, e202318210.

(38) Jahn, H. A.; Teller, E. Stability of polyatomic molecules in degenerate electronic states. I. Orbital degeneracy. *Proc. Roy. Soc*. *London A* **1937**, *161*, 220-235.

(39) Thiele, J.; Balhorn, H. Über einen chinoïden kohlenwasserstoff. *Chem. Ber.* **1904**, *37*, 1463-1470.

(40) Tschichibabin, A.E. Über einige phenylierte derivate des *p,p*-ditolyls. *Chem. Ber.* **1907**, *40*, 1810-1819.

(41) Müller, E.; Pfanz, H. Über biradikaloide terphenylderivate. *Chem. Ber.* **1941**, *74*, 1051-1074.

(42) Müller, E.; Hermann, P. Über ein biradikaloides quterphenylderivat. *Chem. Ber.* **1941**, *74*, 1075-1083.

(43) Trinquier, G.; Malrieu, J.-P. Kekulé versus Lewis: when aromaticity prevents electron pairing and imposes polyradical character. *Chem. Eur. J*. **2015**, *21*, 814-828.

(44) Trinquier, G.; Malrieu, J.-P. Predicting the open-shell character of polycyclic hydrocarbons in terms of Clar sextets. *J. Phys. Chem. A* **2018**, *122*, 1088-1103.

(45) Kuriakose, F.; Commodore, M.; Hu, C. *et al.* Design and synthesis of Kekulè and non-Kekulè diradicaloids *via* the radical periannulation strategy: the power of seven Clar's sextets. *J. Am. Chem. Soc.* **2022**, *144*, 23448-23464.

(46) Grover, G.; Tovar, J. D.; Kertesz, M. Quinonoid versus aromatic π-conjugated oligomers and polymers and their diradical characters. *J. Phys. Chem. C* **2022**, *126*, 5302-5310.

(47) Ortiz, R.; Boto, R. A.; García-Martínez, N.; Sancho-García, J. C.; Melle-Franco, M.; Fernández-Rossier, J. Exchange rules for diradical π-conjugated hydrocarbons. *Nano Letters*, **2019**, *19*, 5991-5997.

(48) Kaur, P.; Ali, M. E. The influence of the radicaloid character of polyaromatic hydrocarbon couplers on magnetic exchange interactions. *Phys. Chem. Chem. Phys.* **2022**, *24*, 13094-13101.

(49) Yu-Qiang, Z.; Shi-Yong, W. Delocalized magnetism in low-dimensional graphene system. *Acta Phys. Sin.* **2022**, *71*, 188101-18.

(50) Plasser, F.; Gerzabek, M. H.; Libisch, F.; Reiter, R.; Burgdörfer, J.; Müller, T.; Shepard, R.; Lischka, H. The multiradical character of one- and two-dimensional graphene nanoribbons. *Angew. Chem. Int. Ed*. **2013**, *52*, 2581-2584.

(51) Hachmann, J.; Dorando, J. J.; Avilés, M.; Chan, G. K.-L.; The radical character of the acenes: A density matrix renormalization group study. *J. Chem. Phys*. **2007**, *127*, 134309-19.

(52) Trinquier, G.; David, G.; Malrieu, J.-P. Qualitative views on the polyradical character of long acenes, *J. Phys. Chem*. *A* **2018**, *122*, 6928-6933.

(53) Das, S.; Wu, J. Polycyclic hydrocarbons with an open-shell ground state. *Physical Sciences Reviews* **2017**, 2016-0109.

(54) Das, S.; Herng, T. S.; Zafra, J. L. *et al.* Fully fuzed quinoidal/aromatic carbazole macrocycles with polyradical character. *J. Am. Chem. Soc*. **2016**, *138*, 7782-7790.

(55) Huang, R.; Phan, H.; Herng, T. S. *et al.* Higher order π-conjugated polycyclic hydrocarbons with open-shell singlet ground state: nonazethrene *vs* nonacene. *J. Am. Chem. Soc*. **2016**, *138*, 10323-10330.

(56) Pariser, R.; Parr, R. A semi-empirical theory of the electronic spectra and electronic structure of complex unsaturated molecules. I. *J. Chem. Phys.* **1953**, *21*, 466-471; II. *J. Chem. Phys.* **1953**, *21*, 767-776.

(57) Pople, J. A. Electron interaction in unsaturated hydrocarbons. *Trans. Faraday Soc.* **1953**, *49*, 1375-1385.

(58) Hubbard, J. Electron correlation in narrow energy bands. *Proc. Roy. Soc. London Ser. A* **1963**, *276*, 238-267.

(59) Ovchinnikov, A. A. Multiplicity of the ground state of large alternant organic molecules with conjugated bonds. *Theor. Chim. Acta* **1978**, *47*, 297-304.

(60) Dirac, P. A. M. On the theory of quantum mechanics. *Proc*. *R*. *Soc*. *London*, *Ser*. *A* **1926**, *112,* 661–677.

(61) Heisenberg W. Zur theorie des ferromagnetismus. *Z. Phys.* **1928**, *49*, 619-636.

(62) Van Vleck, J. H. *The theory of electric and magnetic susceptibilities*, Clarendon Press: Oxford, 1932.

(63) Maynau, D.; Said, M.; Malrieu, J.-P. Looking at chemistry as a spin-ordering problem. *J. Am. Chem. Soc*. **1983**, *105*, 5244-5252.

(64) Said, M.; Maynau, D.; Malrieu, J.-P.; Garcia Bach, M. A. A nonempirical Heisenberg Hamiltonian for the study of conjugated hydrocarbons. Ground-state conformational studies. *J. Am.. Chem. Soc.* **1984**, *106*, 571-579.

(65) Lieb, E. H. Two theorems on the Hubbard model. *Phys. Rev. Lett.* **1989**, *62*, 1201-1204.

(66) Malrieu, J.-P.; Ferré, N.; Guihéry, N. Magnetic properties of conjugated hydrocarbons from topological Hamiltonians. In Challenges in Computational Chemical Physics, Vol. 22; Chauvin, R.; Lepetit, C.; Silvi, B.; Alikani, E. Eds; Applications of Topological Methods in Molecular Chemistry; Springer: Heidelberg, 2016; pp 361-395.

(67) Longuett-Higgins, H. C. Some studies in molecular orbital theory. I. Resonance structures and molecular orbitals in unsaturated hydrocarbons. *J. Chem. Phys.* **1950**, *18*, 265-274.

(68) L. Salem *The molecular orbital theory of conjugated systems*, Benjamin Inc.; New York, 1966.

(69) Calzado, C. J.; Cabrero, J.; Malrieu, J.-P.; Caballol, R. Analysis of the magnetic coupling in binuclear complexes. I. Physics of the coupling. *J. Chem. Phys.* **2002**, *116*, 2728– 2747.

(70) Mahaffy, P. G.; Wieser, J. D.; Montgomery, L. K. An electron diffraction study of *p*-xylylene. *J. Am. Chem. Soc*. **1977**, *99*, 4514-4515.

(71) Guihéry, N.; Maynau, D.; Malrieu, J.-P. From quinoidal to diradical structure in substituted *n-para*-xylylene molecules. A Heisenberg Hamiltonian study. *Chem. Phys. Lett*., 1996, *248,* 199-206.

(72) Angeli, C.; Malrieu, J.-P. Aromaticity: an ab initio evaluation of the properly cyclic delocalization energy and the π-delocalization energy distortivity of benzene. J. Phys. Chem. A **2008**, *112*, 11481-11486.

(73) Frisch, M. J. *et al.*, Gaussian 09, Revision D.01; Gaussian, Inc.: Wallingford, CT, 2013.

(74) Zhao, Y.; Truhlar, D. G. Density functional for spectroscopy: no long-range self-interaction error, good performance for Rydberg and charge-transfer states, and better performance on average than B3LYP for ground states. *J. Phys. Chem. A* **2006**, *110*, 13126-13130.

(75) Valero, R.; Costa, R.; de P. R. Moreira, I.; Truhlar, D.; Illas, F. Performance of the M06 family of exchange-correlation functionals for predicting magnetic coupling in organic and inorganic molecules. *J. Chem. Phys.* **2008**, *128*, 114103-8.

(76) Yamanaka, S.; Okumura, M.; Nakano, M.; Yamaguchi, K. EHF theory of chemical reactions. Part 4. UNO CASSCF, UNO CASPT2 and R(U)HF coupled-cluster (CC) wavefunctions. *J. Mol. Struct. THEOCHEM* **1994**, *310*, 205-218.

(77) David, G.; Ferré, N.; Trinquier, G.; Malrieu, J.-P. Improved evaluation of spin polarization energy from broken -symmetry calculations. *J. Chem. Phys.* **2020**, *153*, 054120-10.

(78) David, G.; Trinquier, G.; Malrieu, J.-P. Consistent spin-decontamination of broken-symmetry calculations of diradicals. *J. Chem. Phys.* **2020**, *153*, 194107-10.

(79) Angeli, C.; Cimiraglia, R.; Evangelisti, S.; Leininger, T.; Malrieu, J.-P. Introduction of *n*-electron valence states for multi-reference perturbation theory. *J. Chem. Phys.* **2001**, *114*, 10252-10264.

(80) Angeli, C.; Cimiraglia, R.; Malrieu, J.-P. *N*-electron valence state perturbation theory: a fast implementation of the strongly contracted variant. *Chem. Phys. Lett.* **2001**, *350*, 297-305.

(81) David, G.; Ben Amor, N.; Zheng, T.; Suaud, N.; Trinquier, G.; Malrieu, J.-P. Difficulty of the evaluation of the barrier height of an open-shell transition state between closed-shell minima: the case of small C_{4n} rings. *J. Chem. Phys.* **2022**, *156*, 224104-14.

(82) Ben Amor, N.; C. Noûs, C..; Trinquier, G.; Malrieu, J.-P. Spin polarization as an electronic cooperative effect. *J. Chem. Phys.* **2020**, *153*, 044118-12.

Table 1. Flake characteristics and calculated relative energies for various solutions.

	flake **5-7**	flake **3-9**
carbon atom count		
polyenic	12	12
polycyclic	28	24
total conjugated	40	36
graphanized [a]	5	12
empirical formula	$C_{45}H_{22}$	$C_{48}H_{30}$
relative energies (kcal/mol)		
closed-shell singlet (vertical)	14.9	13.3
closed-shell singlet	10.2	9.0
triplet	1.0	0.9
BS m_s=0 (vert. closed-shell)	3.9	3.7
BS m_s=0	0.	0.
$<S^2>$	1.13	1.13

[a] CH or CH_2 saturated groups introduced for hole filling, or to prevent clashing between close CH bonds.

Table 2. Mean values of CC bond lengths within relevant subsets.[a]

		BS m_s=0		cl.-sh. singlet	
subsets	*N*	mean	std. dev.	mean	std. dev.
flake **5-7**					
short polyene	6	1.410	0.027	1.406	0.032
long polyene	8	1.408	0.027	1.406	0.038
aromatic group 1	12	1.408	0.020	1.407	0.018
aromatic group 2	12	1.408	0.020	1.415	0.032
total conjugated	46	1.410	0.024	1.410	0.030
flake **3-9**					
short polyene	4	1.422	0.018	1.418	0.033
long polyene	10	1.410	0.028	1.408	0.034
aromatic group 1	12	1.404	0.015	1.402	0.011
aromatic group 2	12	1.404	0.015	1.413	0.033
total conjugated	40	1.411	0.024	1.411	0.030

[a] In Å; *N* is the number of conjugated CC bonds within each set.

Table 3. Characteristics and relative energies for diradicaloid flakes.

	flake **5-5**	flake **3-7**
carbon atom count		
polyenic	10	10
polycyclic	28	24
total conjugated	38	34
graphanized [a]	4	9
empirical formula	$C_{42}H_{20}$	$C_{43}H_{26}$
relative energies (kcal/mol)		
closed-shell singlet (vertical)	3.0	4.8
closed-shell singlet	2.5	4.0
triplet	4.5	2.5
BS m_s=0 (vert. closed-shell)	0.5	0.7
BS m_s=0	0.	0.
$<S^2>$	0.79	0.94

[a] CH or CH_2 saturated groups introduced for hole filling, or to prevent clashing between close CH bonds.

Table 4. Mean values of CC bond lengths within relevant subsets for diralicaloid flakes. [a]

		BS m_s=0		cl.-sh. singlet	
subsets	*N*	mean	std. dev.	mean	std. dev.
flake **5-5**					
polyene	6	1.408	0.023	1.404	0.016
aromatic group	12	1.409	0.021	1.411	0.024
total conjugated	44	1.410	0.024	1.410	0.024
flake **3-7**					
short polyene	4	1.420	0.016	1.414	0.009
long polyene	8	1.408	0.025	1.404	0.016
aromatic group 1	12	1.404	0.016	1.407	0.011
aromatic group 2	12	1.404	0.016	1.407	0.033
total conjugated	38	1.410	0.023	1.410	0.022

[a] In Å; *N* is the number of conjugated CC bonds within each set.

Table5. Combination rules for the lengths of the two odd polyenyl chains.[a]

	entangled	diradicaloid
polyene-1 polyene-2	*4n - 1* *4m + 1*	*4n - 1* *4m - 1*
polyene-1 polyene-2		*4n + 1* *4m + 1*
total polyenes difference polyenes	*4p* *4p + 2*	*4p + 2* *4p*
length of the loop over the entire system [b]	*4k + 2*	*4k*

[a] Integers *n,m,p,k* refer to the number of polyenic conjugated carbon atoms.

[b] This annulene length takes into account that, by construction, each aromatic bridge contributes an even number of conjugated centers to the path.

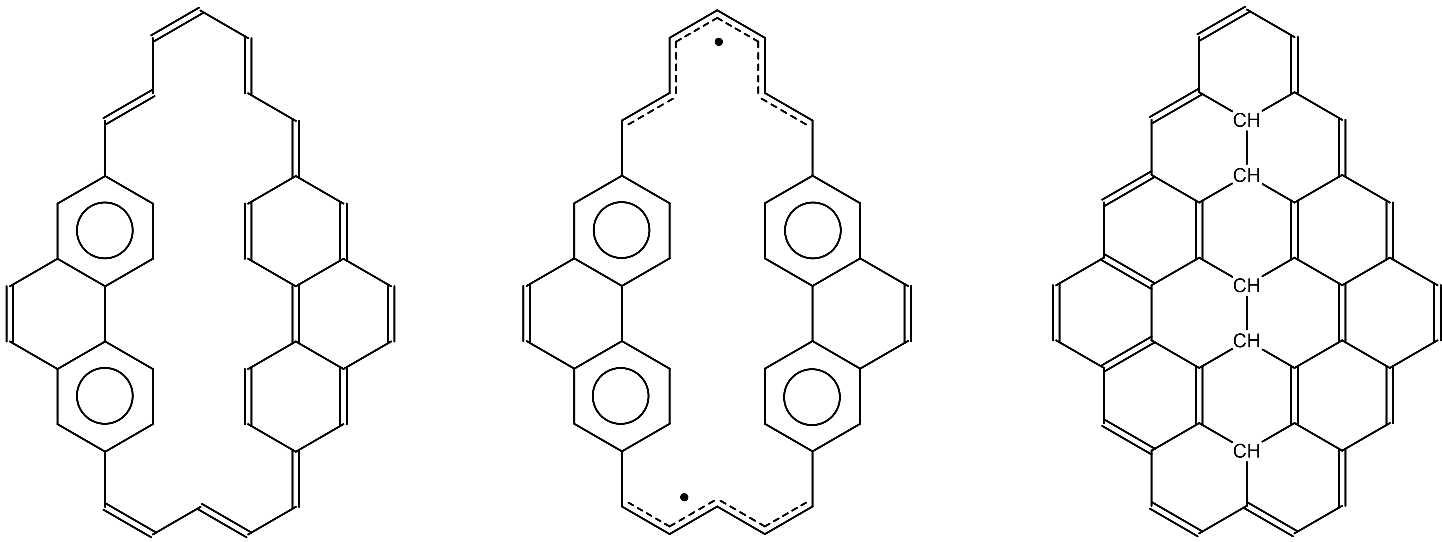

flake **5-7**

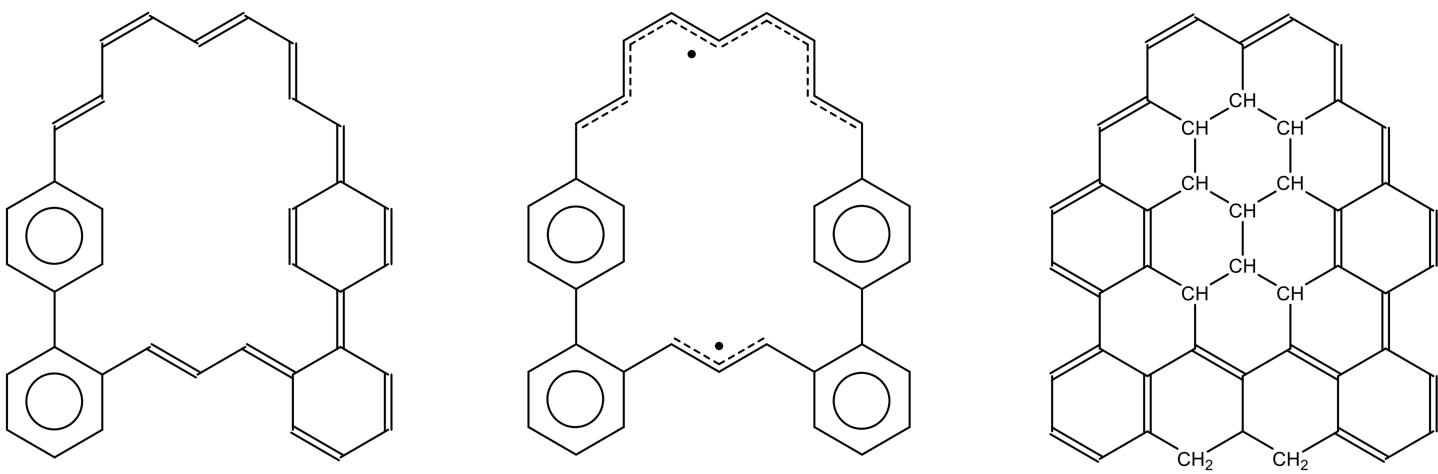

flake **3-9**

Figure 1. The two conjugated hydrocarbon flakes addressed in this study. Left: closed-shell bond pairing Kekulé arrangement; middle: open diradical form, with the two polyenyl chains and maximum aromatic rings; right: the partly graphanized forms, expected to relieve steric hindrance, that were actually studied.

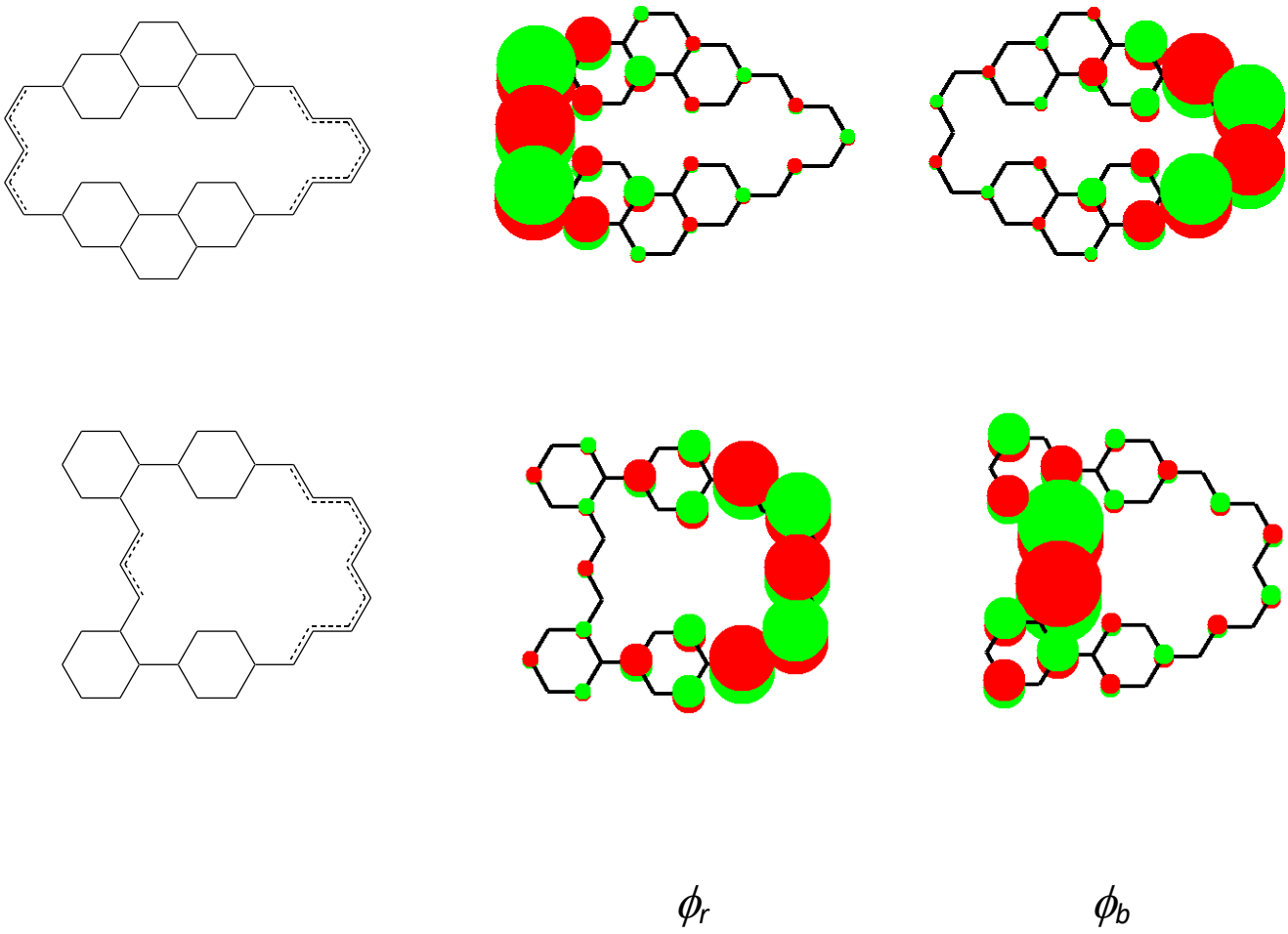

Figure 2. The set of SOMOS, as arising from simple HMO calculations on flakes **5-7** (top) and **3-9** (bottom). Here, colors only reflect wavefunction phases, regardless of any graph coloring considerations.

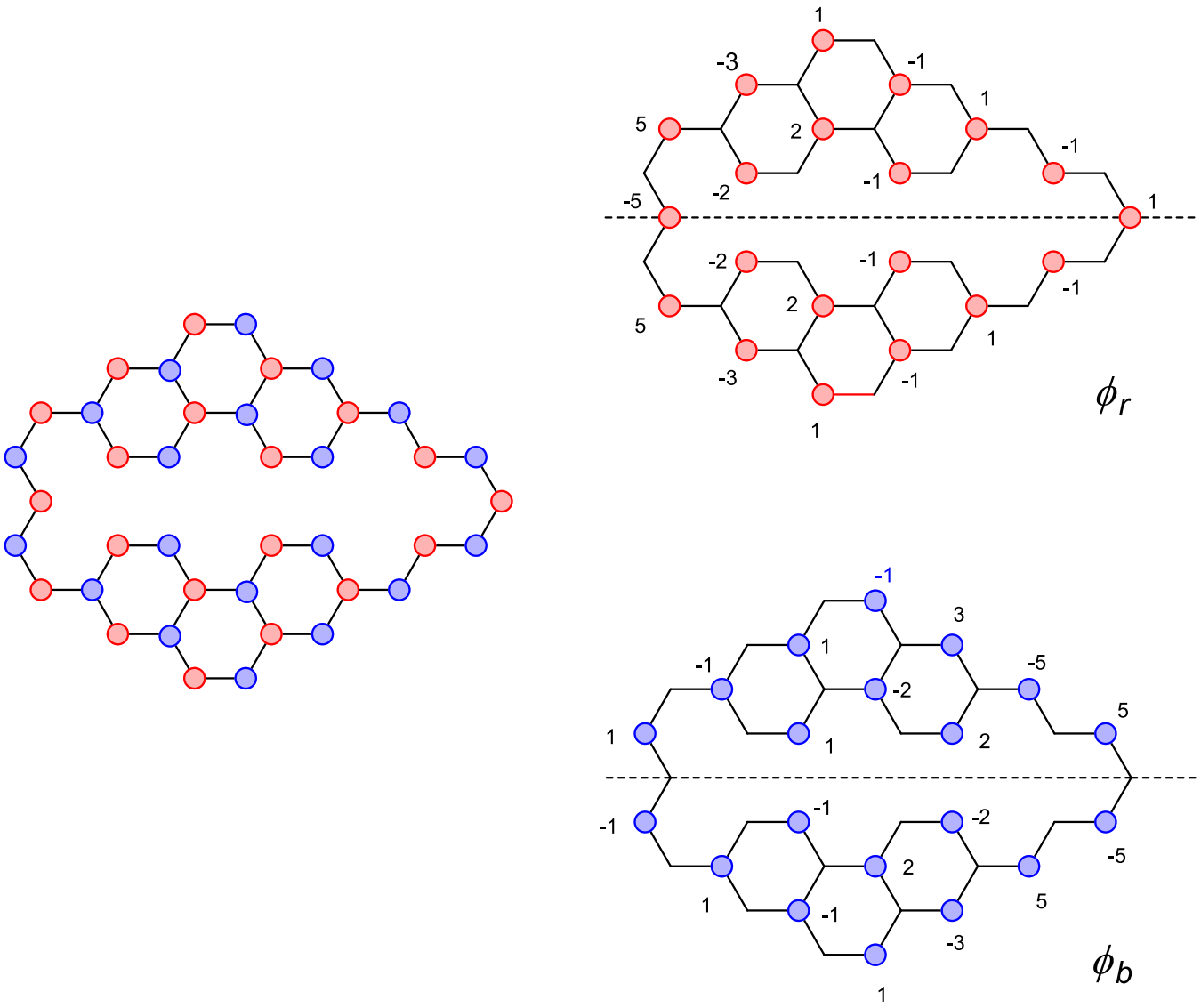

Figure 3. Grouping the colors in flake **5-7**. Left: making explicit the chromatic number of two. Right: the two SOMOS, with schematized color and symmetry properties, and handwave-obtained integer coefficients.

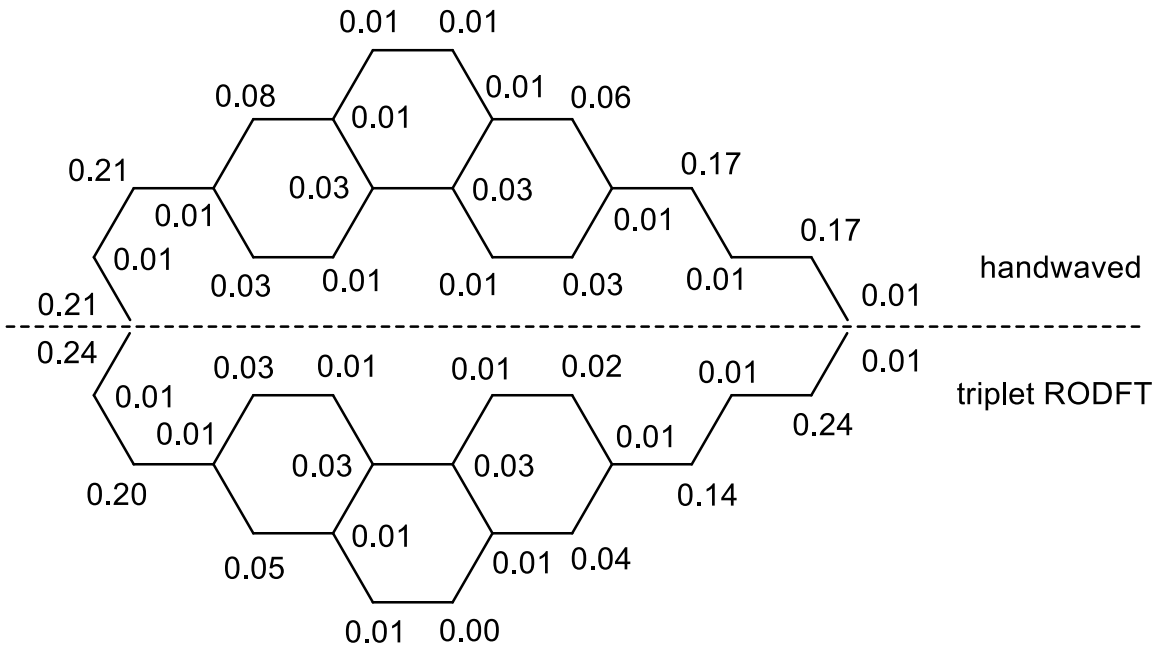

Figure 4. Conparring the handwave-obtained coefficients, suitably normalized and summed over the two SOMOs of flake **5-7** (top) with RODFT-calculated total spin densities in the triplet state of the flake (bottom).

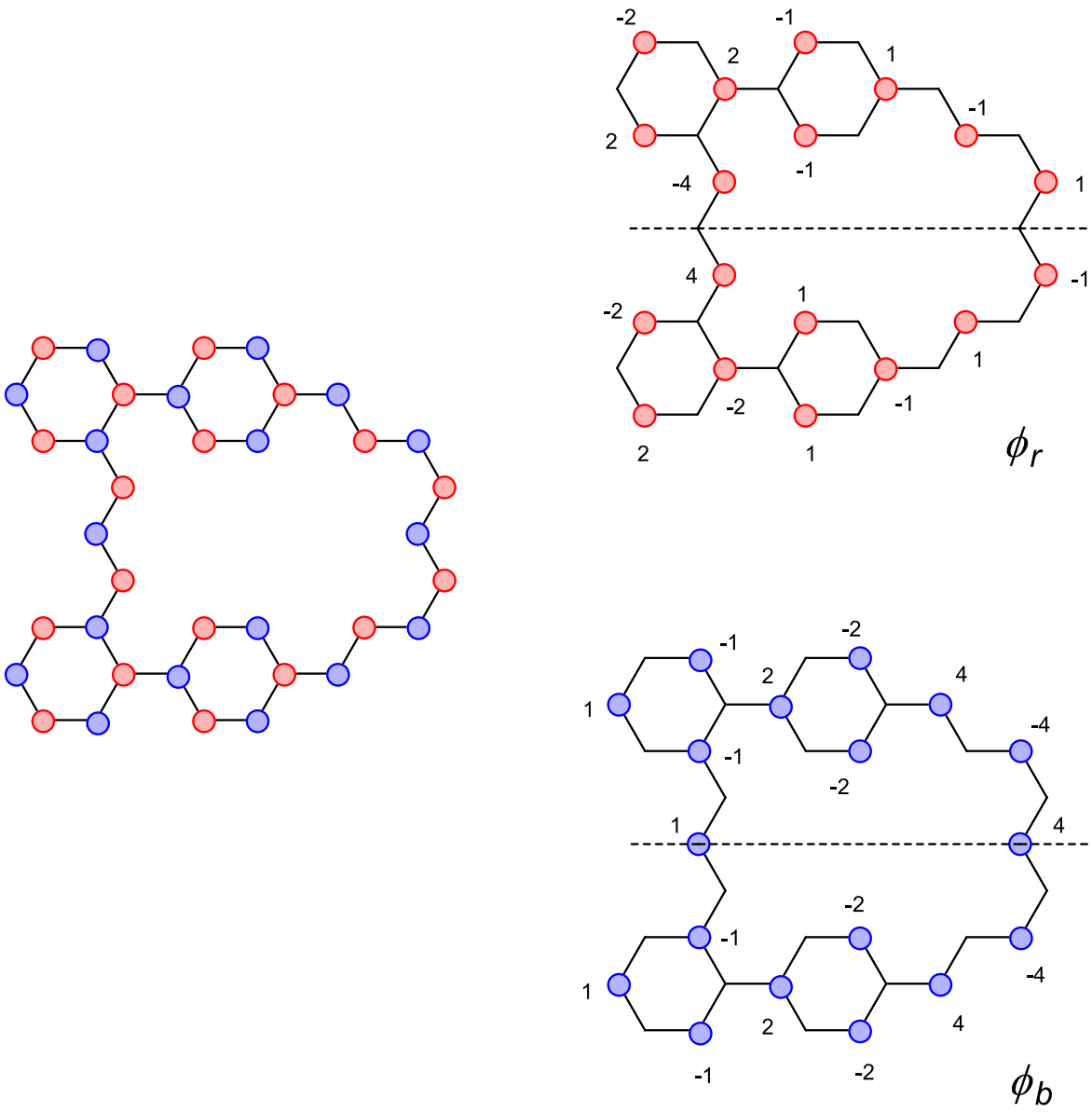

Figure 5. Grouping the colors in flake **3-9**. Letf: making explicit the chromatic number of two. Right: the two SOMOS, with schematized color and symmetry properties, and handwave-obtained integer coefficients.

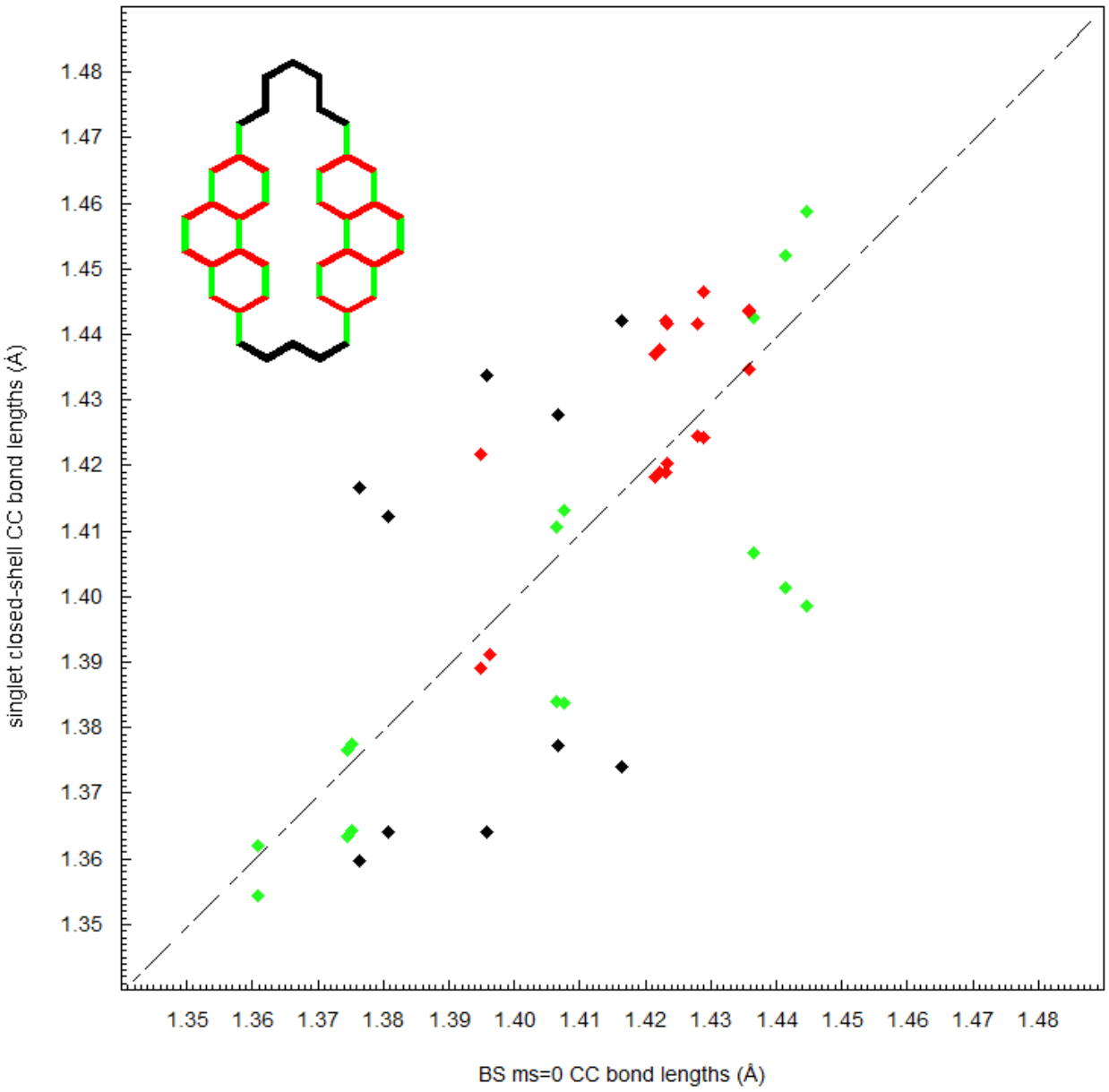

Figure 6. Comparing the calculated CC bond lengths in flake **3-9**. Abscissa refers to the diradical geometry, ordinate to the closed-shell geometry. Black points correspond to polyene bonds, red points to oblique aromatic bonds, green points to vertical aromatic bonds.

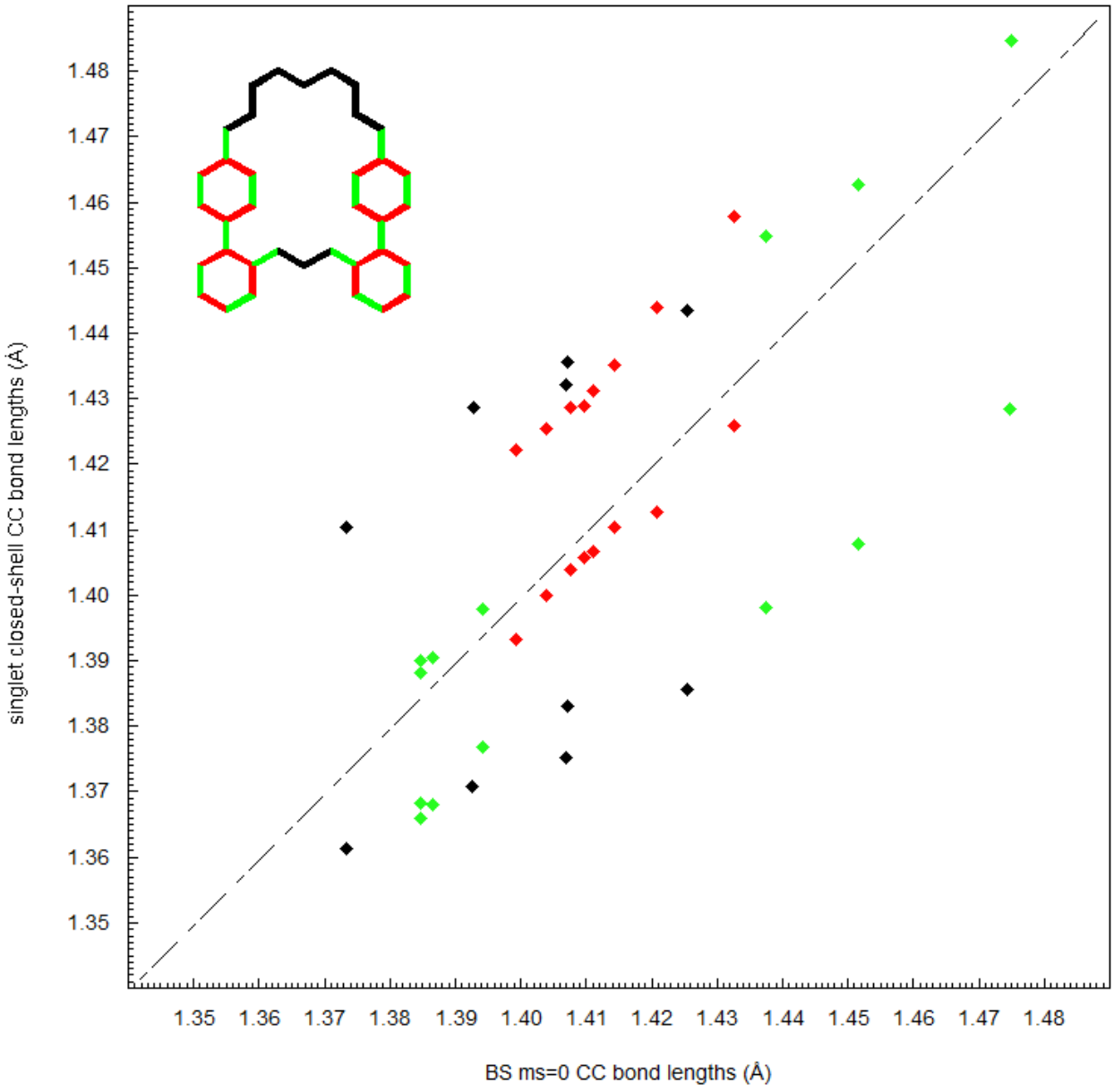

Figure 7. Comparing the calculated CC bond lengths in flake **3-9**. Abscissa refers to diradical geometry, ordinate to closed-shell geometry. Black points correspond to polyene bonds, red points to oblique aromatic bonds, green points to vertical aromatic bonds.

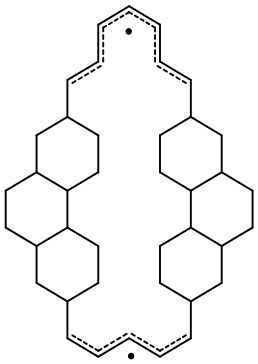

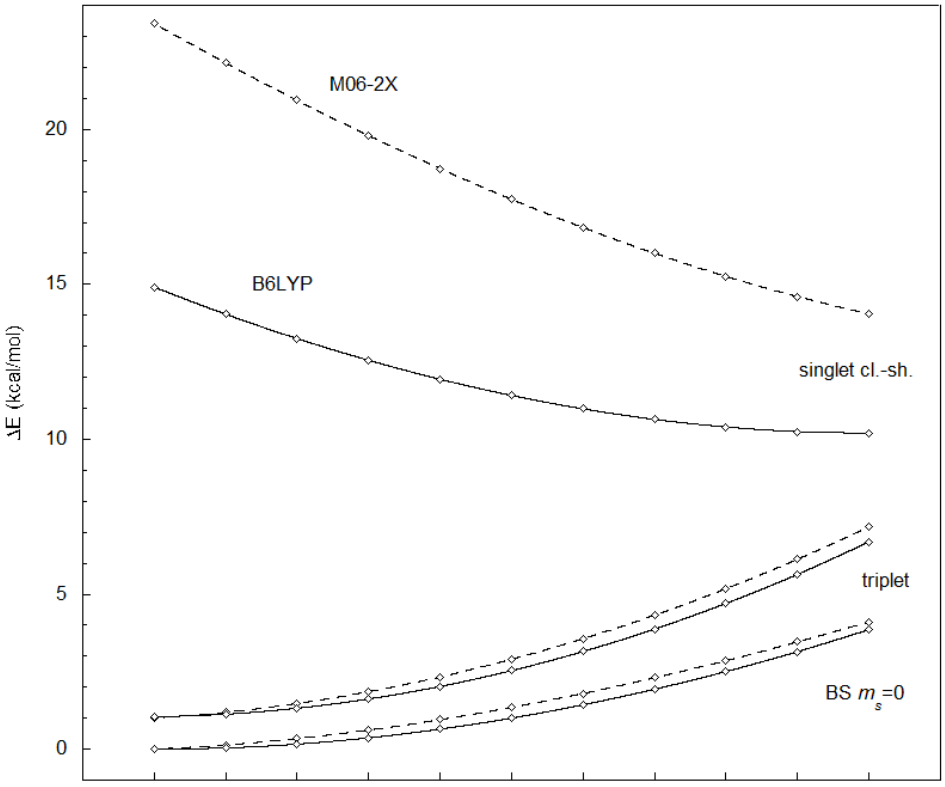

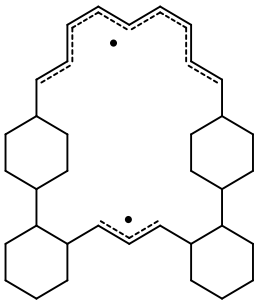

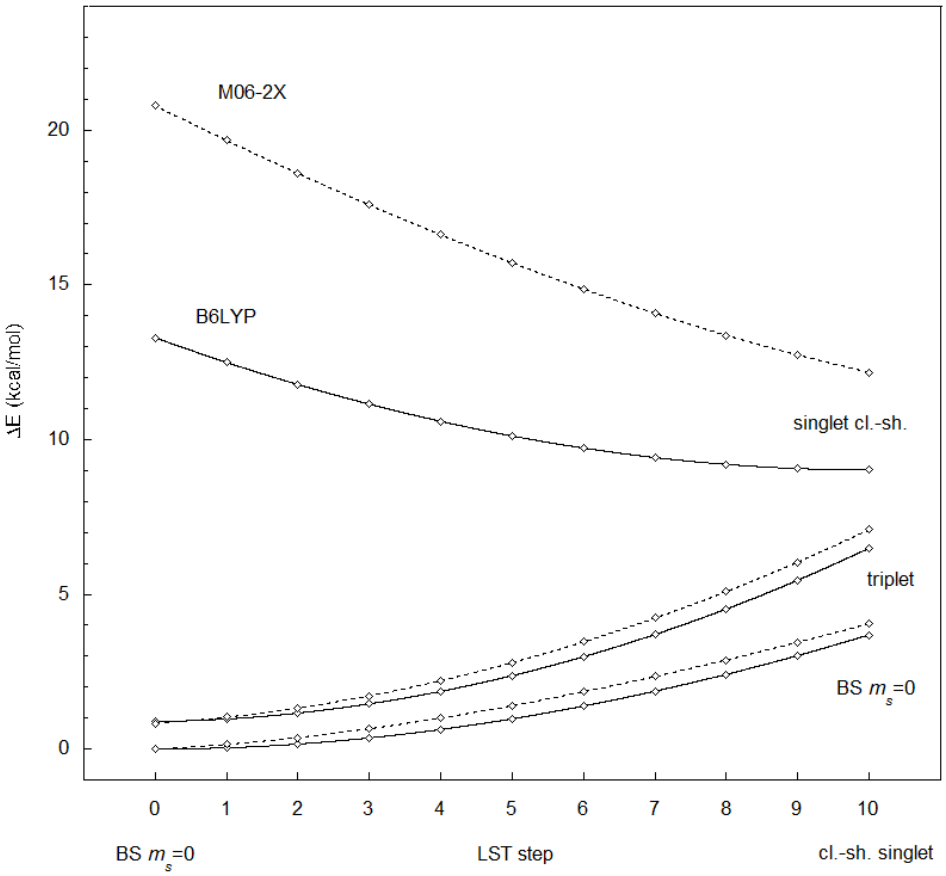

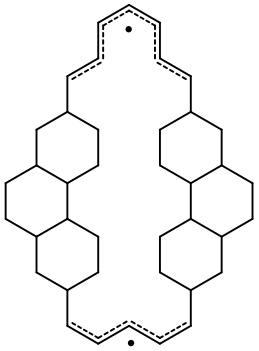

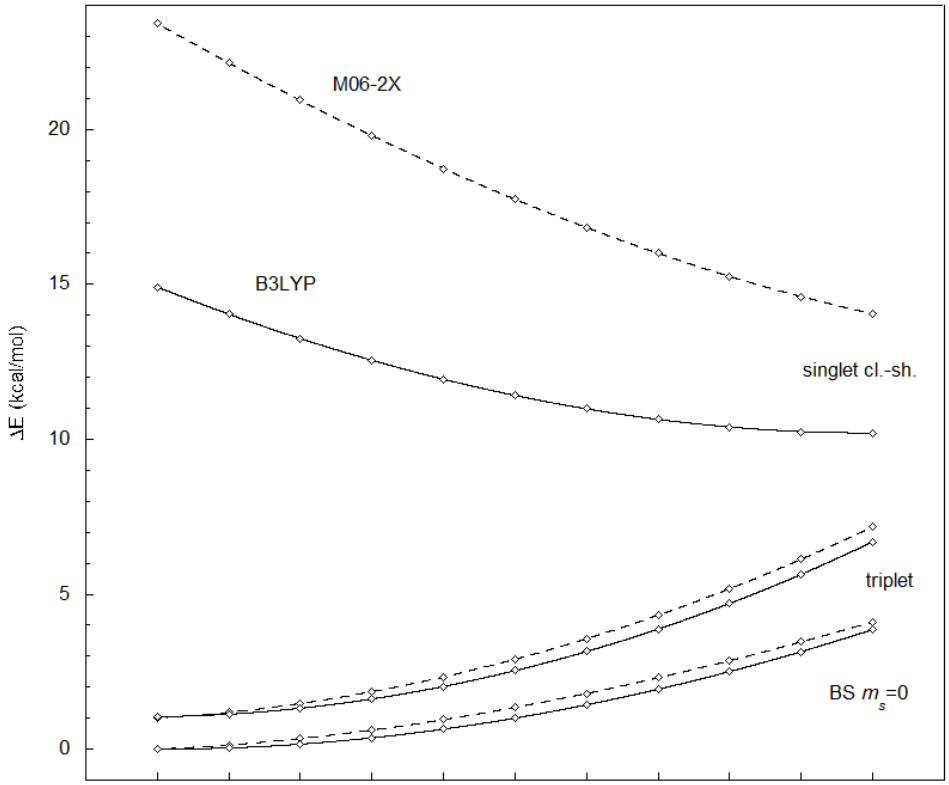

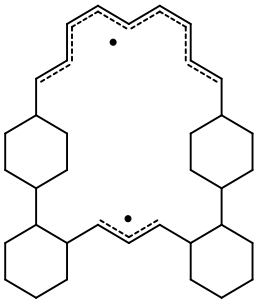

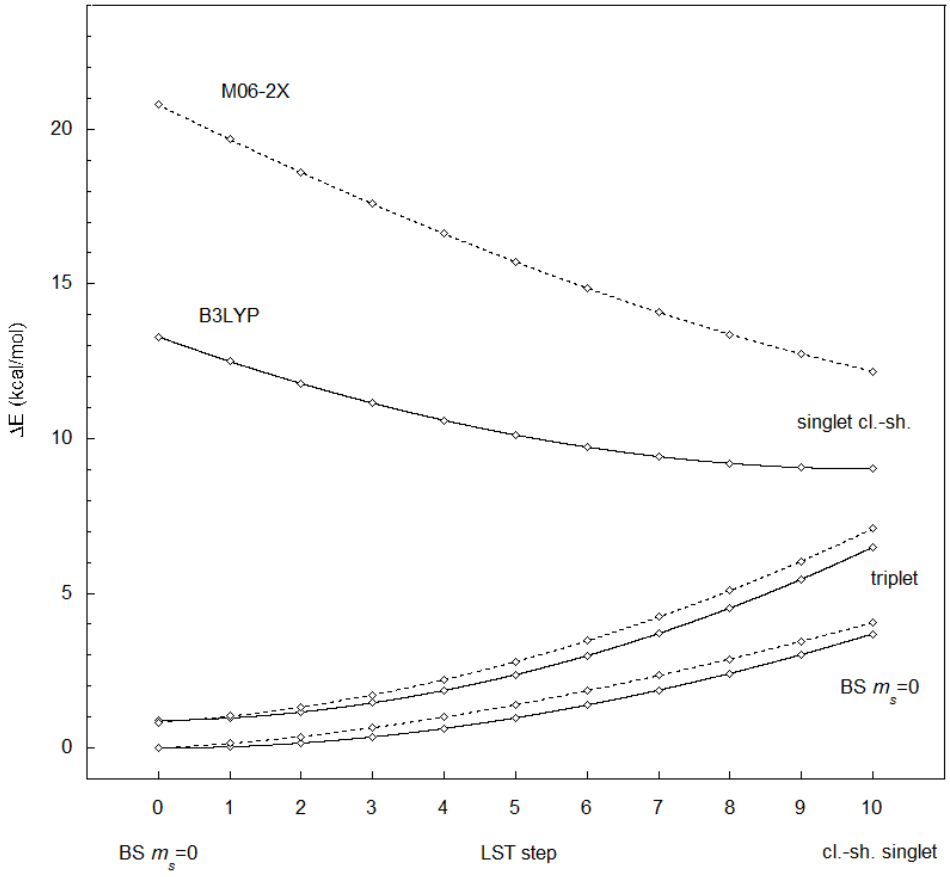

Figure 8. DFT-calculated energies along the linear synchronous transits from BS m_S=0 geometries to closed-shell ones. Comparison of functionals B3LYP (full lines) and MO62X (dashed lines).

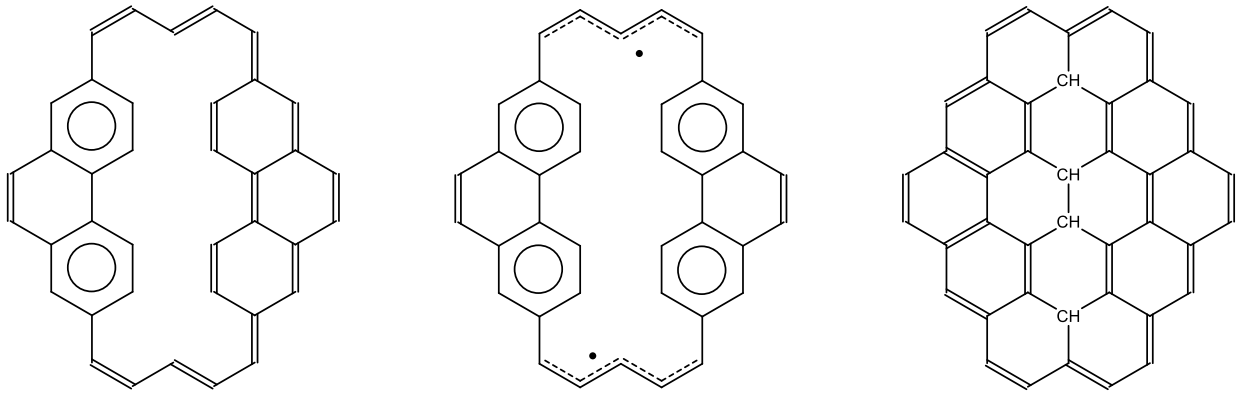

flake **5-5**

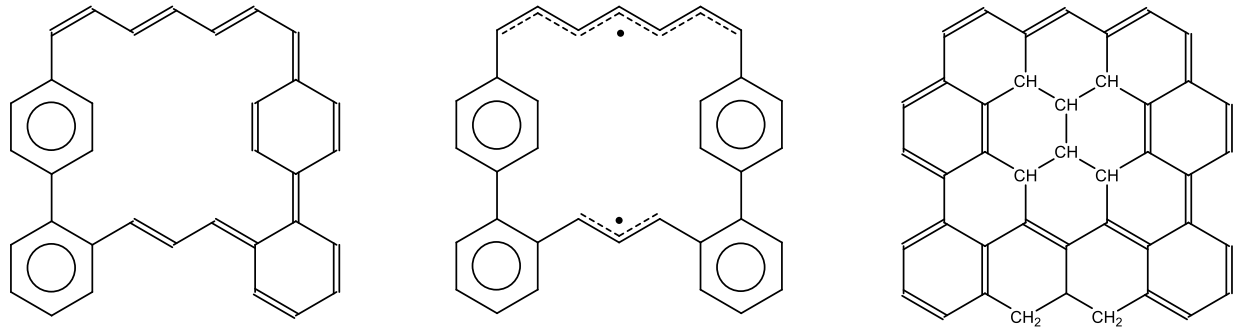

flake **3-7**

Figure 9. Diradicaloids alternatives addressed in this study. Same comments as in Figure 1.

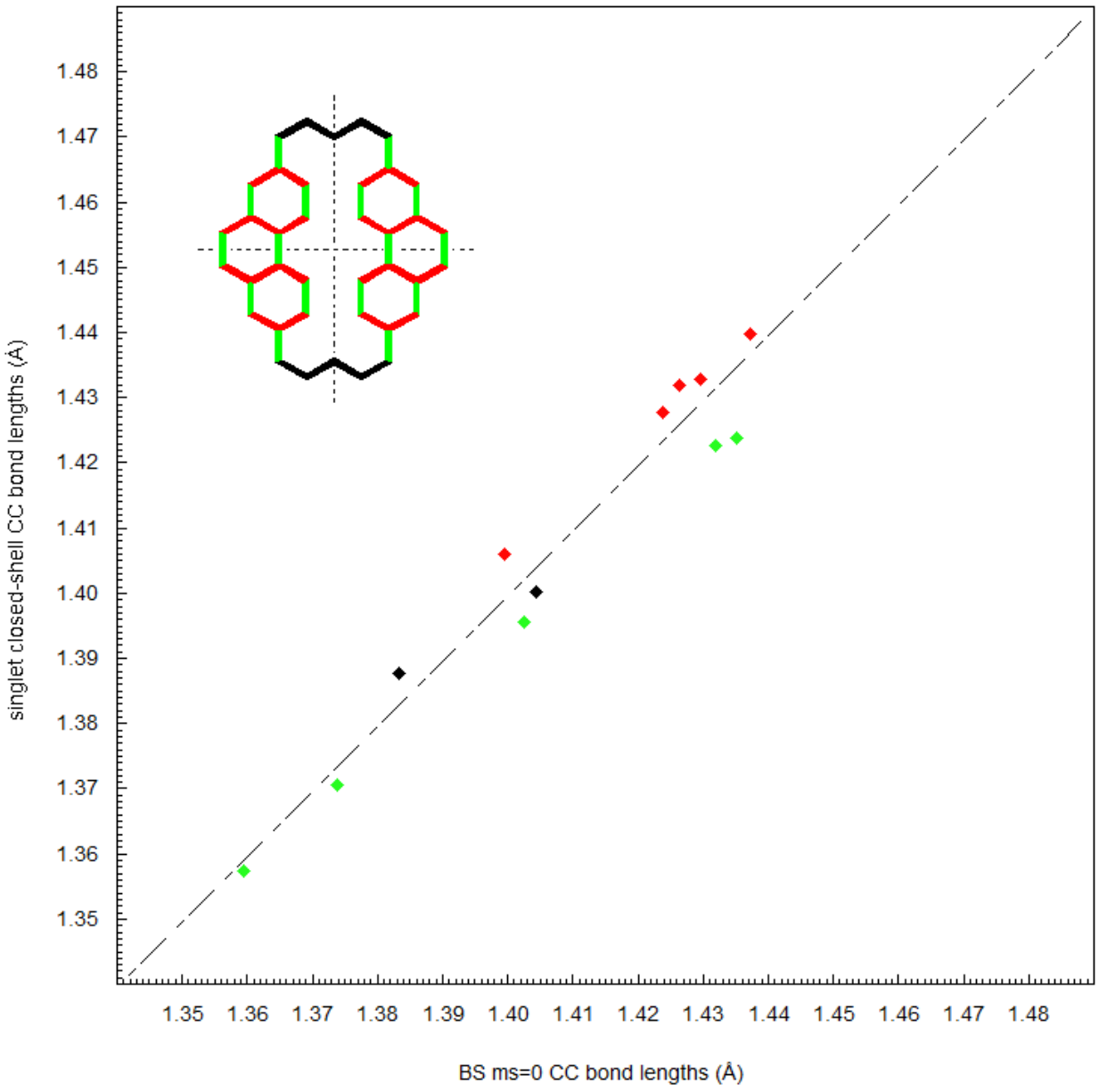

Figure 10. Comparing calculated CC bond lengths in flake **5-5**. Abscissa refers to diradical geometry, ordinate to closed-shell geometry. Black points correspond to polyene bonds, red points to oblique aromatic bonds, green points to vertical aromatic bonds.

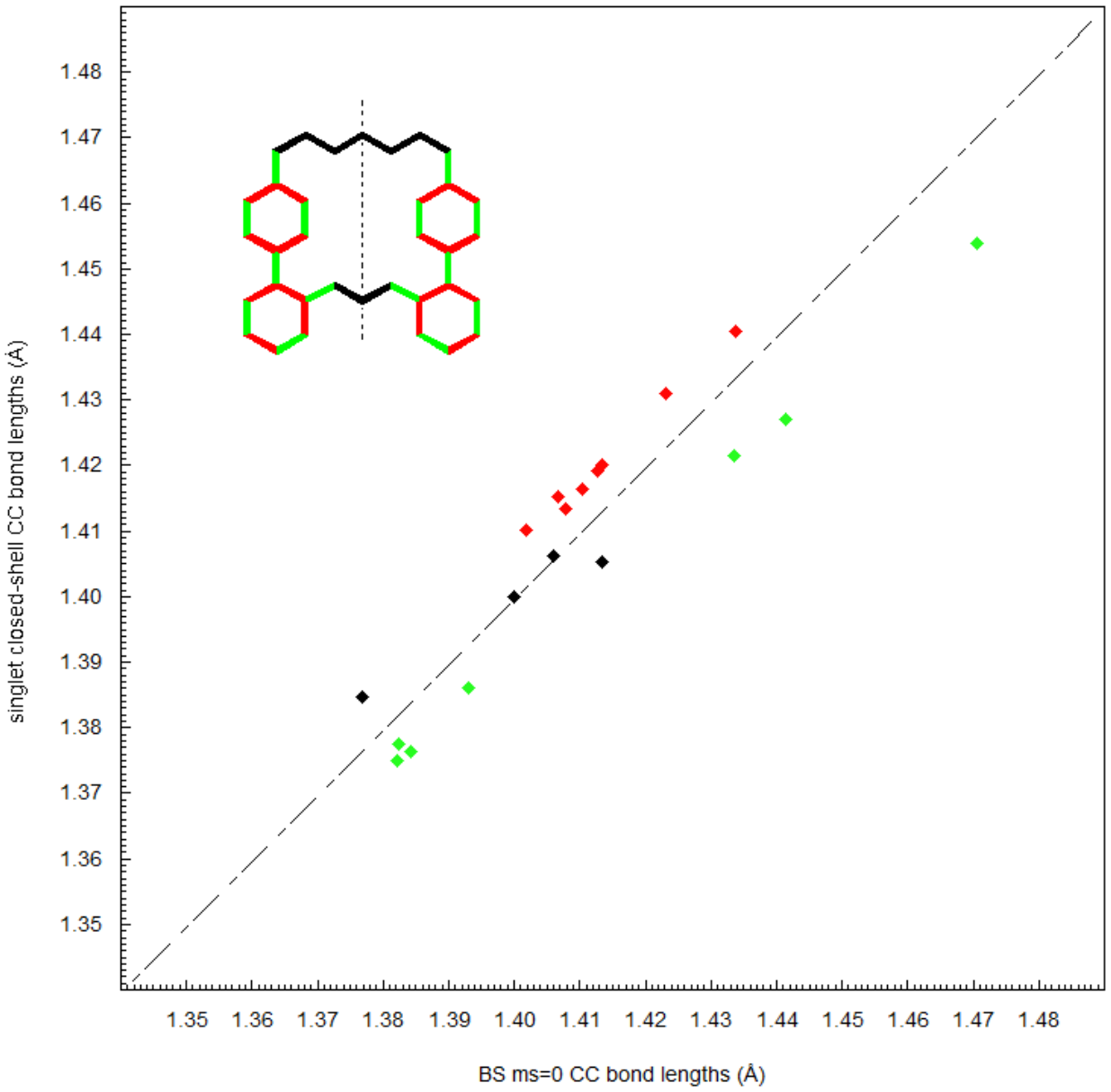

Figure 11. Comparing calculated CC bond lengths in flake **3-7**. Abscissa refers to diradical geometry, ordinate to closed-shell geometry. Black points correspond to polyene bonds, red points to oblique aromatic bonds, green points to vertical aromatic bonds.

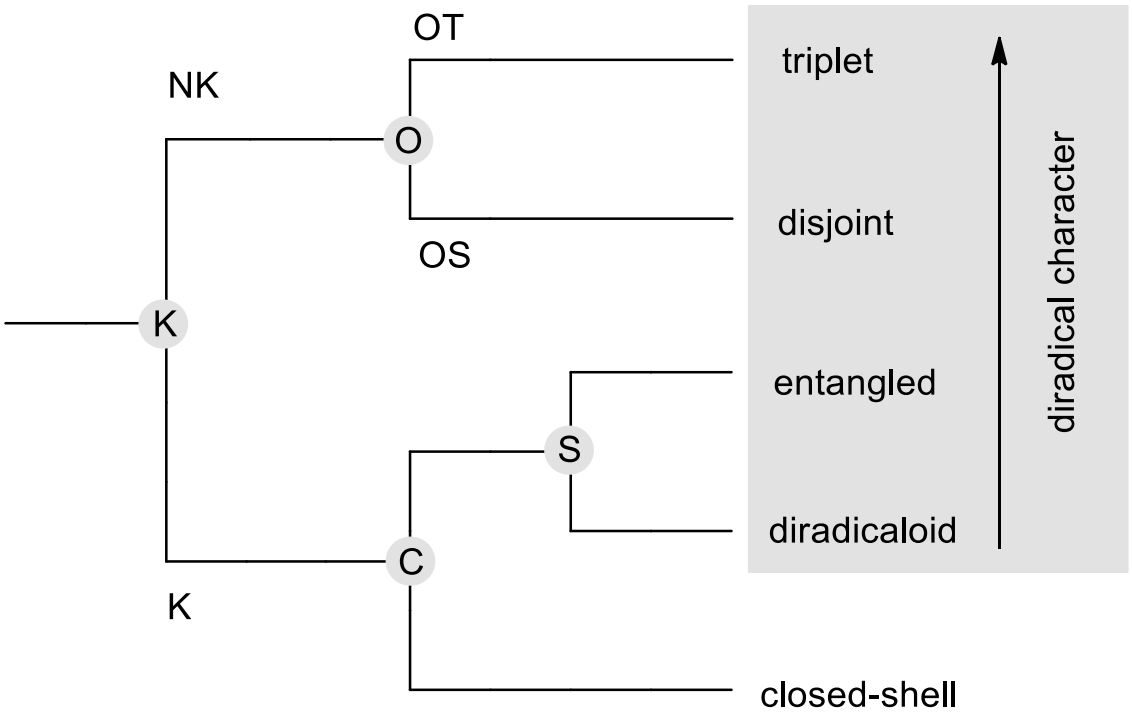

Figure 12. An attempt to categorize even alternate conjugated hydrocarbons with respect to shell opening. Bifurcation points correspond to the following alternatives. “K” refers to on-bond electron pairing, giving either Kekulé (K) or non-Kekulé (NK) structures; “C”, refers to spin instability, reflecting an opening induced by Clar-Chichibabin type driving force; “S” refers to strict SOMO degeneracy; “O” refers to Ovchinnikov’s criterion, according to which a diradical is prone to be singlet (OS) or triplet (OT).